Ocean and Coastal Management 230 (2022) 106367

Contents lists available at ScienceDirect

Ocean and Coastal Management

journal homepage: www.elsevier.com/locate/ocecoaman

# The lower shoreface of the Dutch coast – An overview

Ad van der Spek[a,b,*], Jebbe van der Werf[b,d], Albert Oost[b,1], Tommer Vermaas[c], Bart Grasmeijer[b], Reinier Schrijvershof[b,e]

[a] Faculty of Geosciences, Utrecht University, P.O. Box 80.115, 3508 TC, Utrecht, the Netherlands
[b] Deltares, Applied Morphology Department, P.O. Box 177, 2600 MH, Delft, the Netherlands
[c] Deltares, Applied Geology and Geophysics Department, P.O. Box 85467, 3508 AL, Utrecht, the Netherlands
[d] Department of Water Engineering & Management, University of Twente, P.O. Box 217, 7500 AE, Enschede, the Netherlands
[e] Department of Environmental Sciences, Wageningen University & Research, P.O. Box 9101, 6700 HB, Wageningen, the Netherlands

ABSTRACT

The lower shoreface, defined here as between about 8 and 20 m water depth, forms the transition between the inner shelf and upper shoreface. Knowledge of lower shoreface hydro- and morphodynamics is essential for coastal management and maintenance.

The shoreface of the Dutch coast is a complex area. It is partly determined by its evolution in the past, whereas present-day processes are influencing or even changing it. The present situation and large-scale anthropogenic supply of sediment will determine its future development.

The shoreface morphology varies along the Dutch coast, depending on the coastal slope and superposition of ridges (central Holland coast) and ebb-tidal deltas (Delta area, Wadden Sea). The architecture of the shoreface-connected ridges off the central Holland coast indicates that they are still active today. The development of most ebb-tidal deltas along the Dutch coast is largely influenced by interventions in the tidal inlets and tidal basins.

The Kustgenese 2.0 Lower Shoreface project comprised both field data collection in 2017 and 2018 and numerical modelling. Field data was collected in study areas at Ameland Inlet, Terschelling and Noordwijk. Sediment cores and multibeam sonar surveys provided information on the Holocene deposits, geomorphology and sediments. Instrumented frames placed at the seabed collected a wealth of process data.

The variation in shoreface composition and morphology is larger than anticipated previously. In general, the lower part of the shoreface consists of older Holocene deposits overlain by an active sand layer that responds to variations in tidal, wave and wind conditions. The deposits at the lower shoreface of Terschelling were comparable to the ebb-delta channel deposits at the ebb-delta front at Ameland Inlet. At Noordwijk, deposits of the Late-Holocene prograded barrier shoreface overlie those of back-barrier tidal channels and river channels. The large-scale morphology of the lower shoreface seems rather stable. Decadal time series show an erosional trend. Small-scale bedforms can change over an interval of days to weeks.

The multibeam surveys revealed unexpected details such as geology-based shoreface irregularities between −12m and −18m that probably act as conduits for downslope currents and sand transport. After a high-energy wave event, more erosional features were discovered that suggest seaward sand transport.

Measured orbital velocities at the seabed at 14–16 m depth reached 1.5 m per second under high-wave events. This caused high sediment mobility under sheet-flow conditions with abundant sediment suspension. It is not clear what this means for the net sand transport at the lower shoreface.

The modelled alongshore-directed sand transport is much larger than the cross-shore transport. The largest transports at the 20m depth contour occurs along the northern part of the Holland coast. Here, transport is parallel to the coast or directed to deeper water. Transports at 20 m depth along the other parts of the coast are directed to shallower water.

The modelled total landward sand transport over the −20m contour is c. 4 million $m^3$ per year and c. 7 million $m^3$ per year over the −16m contour. This suggests a yearly erosion of c. 4 million $m^3$ in-between, in case of no alongshore transport gradients.

The results of the sand transport calculations imply a net landward sediment transfer that needs to be further tested against the morphological changes in the shoreface.

## 1. Introduction

### 1.1. The Dutch lower shoreface

The shoreface of a coastline extends from the limit of wave runup on the beach face seaward, to the limit of effective wave influence on the seabed morphology. The offshore limit depends on time scales (Cowell et al., 1999). It can be divided into an upper shoreface dominated by surf-zone processes and a lower shoreface that evolves on much longer time scales (centuries to millennia). The transport of sand over the

* Corresponding author. Faculty of Geosciences, Utrecht University, P.O. Box 80.115, 3508, TC, Utrecht, the Netherlands.
E-mail address: ad.vanderspek@deltares.nl (A. van der Spek).
[1] Present address: Staatsbosbeheer, P.O. Box 2, 3800 AA, Amersfoort, The Netherlands.

https://doi.org/10.1016/j.ocecoaman.2022.106367
Received 17 May 2021; Received in revised form 23 August 2022; Accepted 5 September 2022
Available online 29 September 2022
0964-5691/

shoreface steers the morphodynamic development of a shoreline. For extensive, recent discussions on shoreface morphodynamics and sediment transport, see Hamon-Kerivel et al. (2020) and Anthony and Aagaard (2020). Wiersma and van Alphen (1988) recognized the shoreface as an important part of the coastline. Its composition reflects the geological history of the coast, its present shape and morphodynamics will determine the coastline's future. Along the Dutch coast, the lower shoreface is defined as the zone between approximately the 8m and 20m depth contours, with typical bed slopes between 1:200 and 1:1000 (van der Werf et al., 2017). The lower shoreface is the zone below the fair-weather wave base, where tidal currents and storm waves dominate. It transitions into the inner shelf.

The knowledge about the Dutch lower shoreface (DLSF) is limited. One of the major unanswered questions is about sand transport: is there a net cross-shore sand transport over the lower shoreface? And if so, is it landwards or seawards and under what conditions? Insight into the sediment fluxes over the lower shoreface is highly relevant for management of the Dutch coast, as one of the major assumptions of the current management is that nourished sediments redistribute over the coastal profile.

This paper focusses on the lower shoreface of the Dutch coast and gives an overview of the Lower Shoreface project within the Kustgenese 2.0 research programme. The project included both an extensive literature review, data collection in three study areas with contrasting settings and numerical modelling. Sediment cores and multibeam sonar surveys provided information on the geomorphology and sediments of the lower shoreface of the Dutch coast. Instrumented frames placed at the seabed collected a wealth of process data. A detailed hydrodynamic model of the DLSF was built and validated with the field measurements, allowing sand transport computations as well.

### 1.2. The Kustgenese 2.0 research programme

The Dutch coast has a total length of c. 350 km and can be divided into three main areas: the Delta coast in the southwest that consists of the engineered distributaries of the rivers Rhine, Meuse and Scheldt, the beach-barrier coast of Holland, and the Wadden coast that consists of barrier islands and tidal inlets fronting back-barrier tidal basins (Fig. 1). The Dutch coastal policy aims for a safe, economically strong and attractive coast. To achieve this, the coast and the shoreface are maintained with regular sand nourishments. The nourished maintenance zone is called 'coastal foundation'. Its offshore boundary is set at the


**Fig. 1.** Overview of the coastal zone of the Netherlands. Indicated are the boundaries of the coastal foundation, the −15m contour, the Delta- Holland- and Wadden coasts, major coastal cities and the Ems and Western Scheldt estuaries.

20m depth contour, while the onshore limit is formed by the landward boundary of the ecologically important dune area and by the tidal inlets. A significant part of the annually nourished volume is placed on the shoreface between 5 m and 8 m depth. Natural processes are assumed to redistribute the sand over the coastal foundation. In 2022 the Dutch Ministry of Infrastructure and Water Management will decide on the future annual nourishment volume, considering the impacts of climate change. The Kustgenese 2.0 (KG2) programme aimed at generating knowledge to support this decision process. The Lower Shoreface project of the KG2 programme ran from 2017 to 2020 and focussed on two main questions:

1. What are possibilities for an alternative offshore boundary of the coastal foundation?
2. How much sediment is required for the coastal foundation to grow with sea-level rise?

These questions at decision-making level address the stability of the shoreface and the exchange of sediments over it. Changes in depth and slope determine the stability of the lower shoreface on decadal timescales. The rate of change depends on driving mechanisms such as waves and currents, on the structure of the subsurface and spatial variation therein, both cross-shore and alongshore, but above all on the net effect of sediment transport over the lower shoreface, during average conditions and events such as storms. To answer the questions above, an accurate and up-to-date understanding of the structure, dynamics and sediment transport over the lower shoreface is necessary.

### 1.3. Objective

The objective of this study is to combine both existing and newly acquired data and information on the geology, sedimentology, sand-transport processes and morphodynamics of the DLSF into an up-to-date overview of the structure of the DLSF and short- and long-term changes therein.

This overview will be the knowledge base that underpins our present understanding of the stability and sediment dynamics of the DLSF and helps in defining the offshore boundary of the coastal foundation and the necessary annual nourishment volume. More background information and definitions are given by van der Werf et al., 2017 and Lodder and Slinger, 2022, this issue.

An easily accessible version for the non-specialist of this overview has been published as *The Kustgenese 2.0 Atlas of the Dutch Lower Shoreface* (van der Spek et al., 2020), which can be downloaded from https://puc.overheid.nl/rijkswaterstaat/doc/PUC_632830_31/1/.

Note that all depths in this paper are given with reference to NAP (Dutch Ordinance Level), which is approximately mean sea level.

## 2. Earlier work

The shoreface of the Dutch coast received extensive attention during the coastal development research project *Kustgenese* (Coastal Genesis), that ran from the mid-1980s to the late 1990s. Comprehensive surveys of coastal bathymetry and geomorphology (van Alphen and Damoiseaux, 1987, 1989), sediment composition and near-surface geology (Niessen and Laban, 1987; Niessen, 1989, 1990) were undertaken. Moreover, both the internal architecture and sediment-composition of, and the processes at the shoreface-connected ridges along the central Holland coast were studied (Van de Meene, 1994; Van de Meene et al., 1996; Van de Meene and van Rijn, 2000a,b). Studies of sediment cores revealed the geology of the present-day shoreface (Beets et al., 1995) and of the mid-Holocene shoreface of the prograded beach barriers along the Holland coast (van der Valk, 1996).

This section gives a short overview of available information on the architecture, morphodynamics, sediment composition, processes and decadal evolution of the Dutch shoreface at the start of the KG2 programme. For a complete inventory the reader is referred to the report by van der Werf et al. (2017). See Fig. 1 for topographical orientation.

### 2.1. Shoreface geology

Summaries of the Holocene evolution of the Dutch coast are presented by Beets et al. (1992) and Beets and van der Spek (2000). Vos et al. (2020) present a series of reconstructed maps of this evolution. Up until 5000 years before present (BP), the coast of The Netherlands showed an overall retreat, mainly due to the rapid rate of sea-level rise (SLR) caused by the melting of the land ice masses of the last glacial period. Around 5000 BP the SLR rate had dropped significantly. Sediment supply, predominantly from reworking of the shallow seabed and erosion of the high-lying Pleistocene relief, was able to fill in the tidal basins, changing them from lagoons into intertidal flats, and subsequently into peat bogs, which resulted in (gradual) closure of the tidal inlets and stabilising of the coastline. The Wadden area is an exception to this, since in the western part there were no tidal basins because of the high-lying Pleistocene and in the eastern part the sediment supply was insufficient to fill in the tidal basins completely. After 5000 BP the Delta, Holland and Wadden coasts showed different evolutions.

The shoreface geology of the Delta coast has not been studied comprehensively. Local studies such as Ebbing and Laban (1996) provide limited insight. The subsurface of the shoreface of the Holland coast has been surveyed extensively with seismics and sediment cores. Moreover, the shoreface deposits of the prograded beach-barrier coast from south of The Hague to Alkmaar have been studied in detail. The shoreface of the Wadden coast has been studied predominantly through seismic surveys, complemented with analyses of sediment cores. The general picture is as follows:

1 The seabed consists of an active sand layer, active meaning that it is mobile due to small-scale bedforms such as megaripples that migrate over the seabed. Reworking by waves under storm conditions is common. This layer consists of brown sand which indicates reworking under oxygen-rich conditions, and is rich in shells.
2 Below the active layer remnants of the transgressive coastal system are found. Coastal retreat causes erosion, predominantly by waves. The retreating shoreline transgressed over its back-barrier, exposing back-barrier deposits at the shoreface. The eroding waves have removed the upper parts of the back-barrier deposits and hence only the lower parts, that are usually cut into the subsurface, have been preserved. In many places along the Dutch coast (from south of Hook of Holland, along the Holland and Wadden coast, to the Ems estuary), the lower parts of the deposits of migrating tidal channels, from both inlet and back-barrier basin, are recognized in seismic surveys and cores.

South of The Hague, channel deposits associated with the Late-Pleistocene and early Holocene river Rhine are found (see van Heteren et al., 2002; and Hijma et al., 2010; for details). The shoreface of the Holland coast between Hook of Holland and IJmuiden has been studied in detail. Beets et al. (1995) demonstrated the variety of deposits to be found here. Rieu et al. (2005) reconstructed the channel patterns of the mid-Holocene tidal basins that occur offshore the area between The Hague and IJmuiden. Van Heteren and van der Spek (2008) described the remnants of the delta of the Old Rhine distributary that is found offshore halfway between The Hague and IJmuiden, whereas van Heteren et al. (2011) explained how the prograding beach barriers were supplied with sand from the eroding lower shoreface.

Seismic surveys along the Wadden coast revealed the migration of predecessors of the present-day tidal inlets (see Sha, 1989b; Sha, 1992; and van Heteren and van der Spek, 2003). The western part of the Wadden Sea is comparatively young since here the top of the Pleistocene deposits was not transgressed before the early Middle Ages. Offshore of this part, predominantly erosional products of Pleistocene deposits (boulder fields) and limited traces of channels occur (Sha et al., 1996).

#### *2.1.1. Shoreface deposits of prograding beach barriers – Holland coast 5000 BP – 2000 BP*

The series of prograded beach barriers between The Hague and Alkmaar allows for detailed study of shoreface deposits. Transects between The Hague and IJmuiden were studied by van Straaten (1965), van der Valk (1996), van der Spek et al. (1999) and Cleveringa (2000). The sediment sequences showed that the shoreline was prograding over eroded tidal basin/tidal channel deposits. The upper shoreface deposits showed the influence of frequent wave activity that decreased with depth. Lower shoreface deposits showed evidence of transport by tidal currents whereas the upper part of the lower shoreface was a relatively quiet environment where bioturbation by benthic organisms dominated. Storm events resuspended shoreface sediments down to the lower shoreface that were subsequently settling from suspension, producing fining-upward sequences with coarse shell layers at their bottom and grading upwards into sand and clay. The completeness of these storm sequences at the lower shoreface were thought to imply that reworking by storm waves at these depths was only an occasional event. These conclusions are summarized in Fig. 2. The validity of this conceptual model of shoreface processes and evolution for the present-day situation needs to be tested.

### *2.2. Shoreface morphology*

Wiersma and van Alphen (1988) described the morphology of the shoreface of the Holland coast between Hook of Holland and Den Helder. They concluded that the shoreface morphology varies considerably along the coast, depending on the (1) coastal slope and (2) the superposition of ridges and tidal deltas. Van Alphen and Damoiseaux (1987) presented a series of 78 shore-normal depth profiles of the shoreface morphology from SW to NE along the Dutch coast, which extended about 20 km offshore with an alongshore spacing of approx. 5 km. The profiles show a relatively flat seabed beneath the 20m depth contour and a sloping shoreface. The shoreface shows a steep upper part with a slope gradient steeper than 1:100 and a lower part with gradients between 1:100 and 1:1000. These authors produced a morphological map of the shoreface of The Netherlands and the adjacent part of the continental shelf, based on both these profiles and depth charts that were constructed between 1977 and 1984 (van Alphen and Damoiseaux, 1987, 1989). This map shows distinct differences between shorefaces of the Delta area, the Holland coast and the Wadden coast (Fig. 3).

#### *2.2.1. Delta area*

The shoreface of the Delta area consists of the contiguous ebb-tidal deltas (ETDs) of the (former) estuaries Western Scheldt, Eastern Scheldt, Grevelingen and Haringvliet (from south to north, see Fig. 3), that are collectively indicated as the *Voordelta*. The ETDs have low-gradient platforms (slopes of less than 1:1000 to 1:100) that are dissected by ebb- and flood-tidal channels and have inter-to supratidal sand bars on top. The gradients of the seaward slopes of the ETDs are ranging from 1:1000 to steeper than 1:100. Only the Eastern Scheldt ETD extends to the 20m depth contour, the others grade into a lower shoreface. Smaller-scale morphological elements such as plateaus and isolated bars, especially along the former island coasts, occur (see Elias

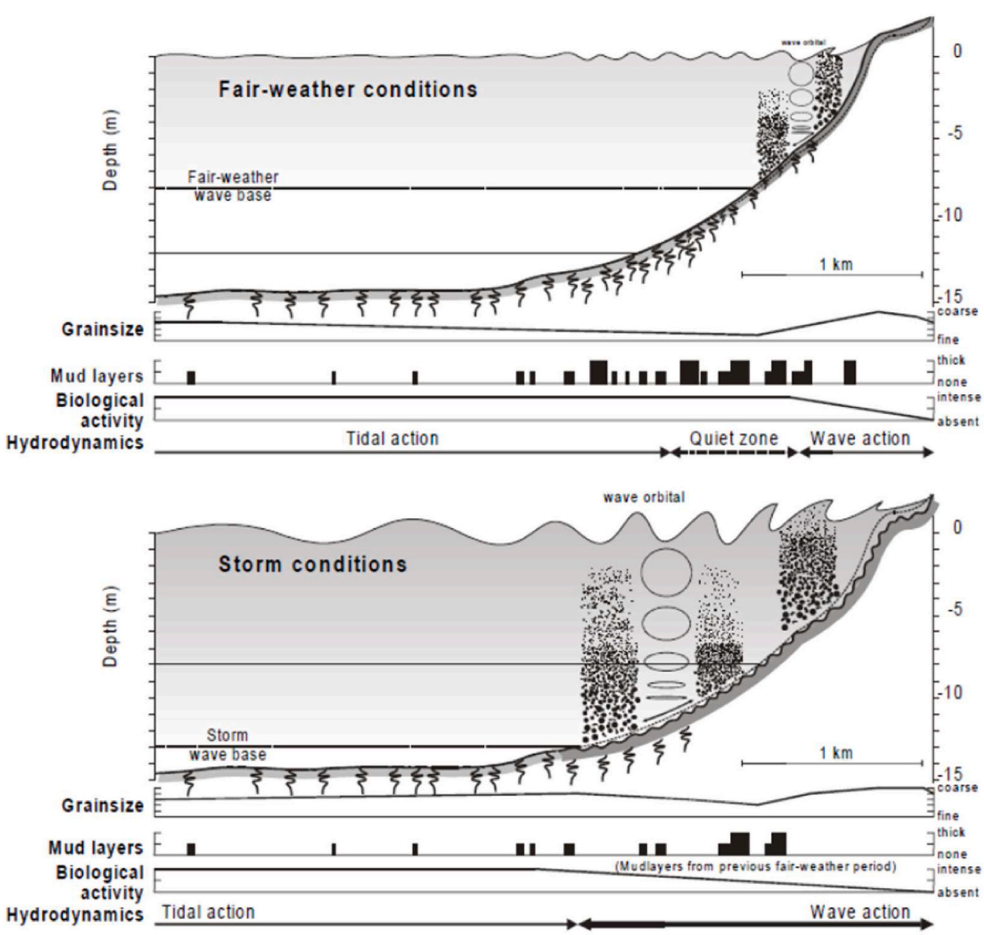


**Fig. 2.** Conceptual model of shoreface processes based on the interpretation of sub-recent shoreface deposits from the Holland coast. From Cleveringa (2000); reproduced with permission.

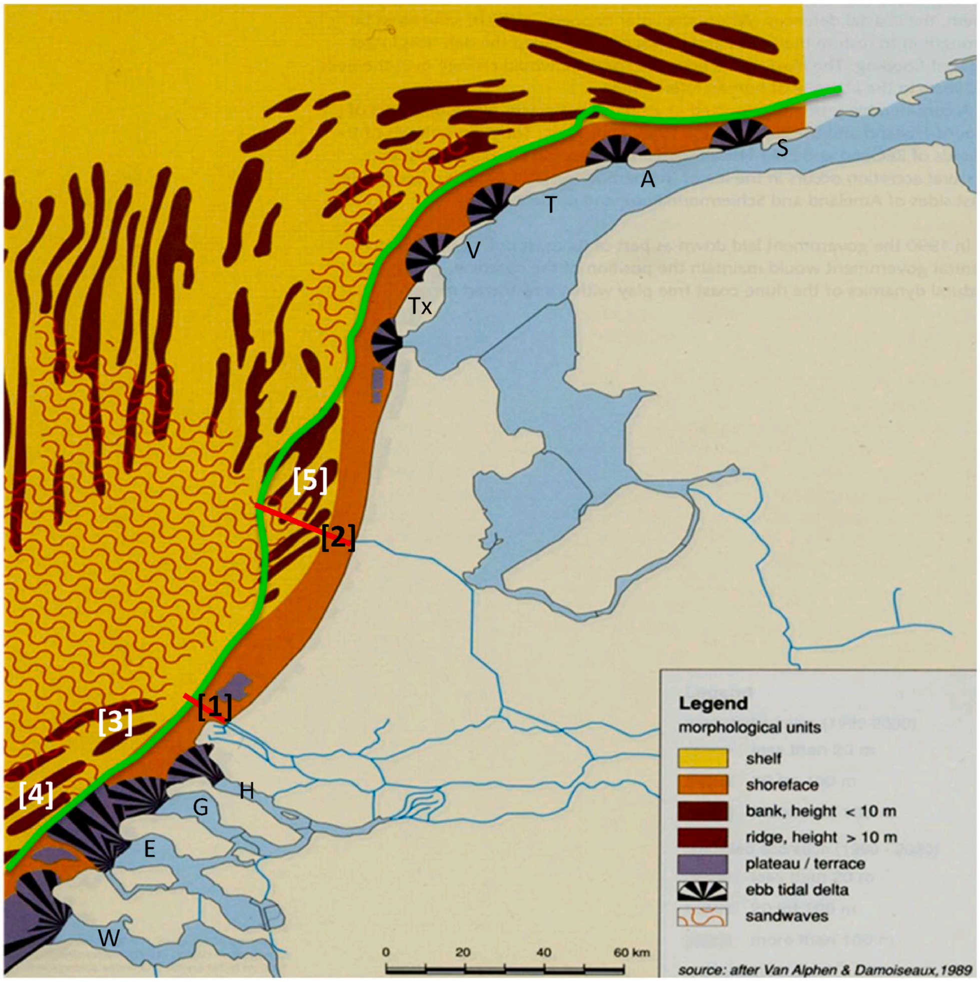


**Fig. 3.** Simplified morphological map of the shoreface of The Netherlands and the adjacent part of the continental shelf. The green line indicates the seaward boundary of the coastal foundation (which roughly follows the 20m depth contour; compare Fig. 1). Indicated are the Maasgeul [1] and IJgeul [2] navigation channels (red lines), the Bollen van Goeree [3] and Zeeland Banken [4] sand ridges, and the shoreface-connected sand ridges at the central Holland coast [5]. The (former) estuaries along the Delta coast (H=Haringvliet; G = Grevelingen; E = Eastern Scheldt; W=Western Scheldt) and the barrier islands of the Wadden coast (Tx = Texel; V=Vlieland, T = Terschelling; A = Ameland; S=Schiermonnikoog) are shown as well. After van Alphen and Damoiseaux (1987).
(Source background map. https://www.arcgis.com/home/webmap/viewer.html?url=https%3A%2F%2Fgeoweb.rijkswaterstaat.nl%2Farcgis%2Frest%2Fservices%2FNoordzeeAtlas%2FNZ_NZA_geomorfologie%2FMapServer&source=sd).

et al., 2017; and van der Spek and Elias, 2021; for details on the evolution of the Voordelta). Offshore of the shoreface, the southwest-northeast running sand ridges of the *Zeeland Banken* and the *Bollen van Goeree* are situated (Fig. 3). The northeastern tips of the Bollen van Goeree ridges connect to the lower shoreface of the Haringvliet ebb-tidal delta. Sand waves do occur in all areas. In the northern part of the Delta area the constructed Maasvlakte 2 sits within the shoreface area. The Maasgeul navigation channel (Fig. 3) separates this area from the Holland coast.

### 2.2.2. *Holland coast*

The shoreface of the continuous, 120 km-long Holland coast consists of a steep surf zone (gradient steeper than 1:100) that is dominated by shore-parallel breaker bars in most places and a less steep lower shoreface (gradient 1:100–1:1000). From Hook of Holland to north of The Hague, the shoreface is up to 8.5 km wide and extends to the −20m contour. Going farther north up to Alkmaar, the shoreface is less than 4 km wide and runs down to the −16m contour. Here, the shoreface is bounded by a series of 10 sand ridges that rise from a flat seabed (slope <1:1000). Four of these ridges connect to the shoreface (see section 2.2.5). Sand waves occur on most of the ridges. In the area with sand ridges the −20m contour lies up to approximately 20 km offshore (Fig. 3). The dredged IJgeul navigation channel dissects this area.

North of Alkmaar, the shoreface widens and extends to the −20m contour again. Here, SW-NE oriented isolated bars occur on the shoreface and it includes two shallow plateaus, the southern of which is called Pettemer Polder. The occurrence of these plateaus is related to Pleistocene relief in the subsurface (de Mulder, 1984). In the north, the shoreface is bounded by the ETD of Texel Inlet.

### 2.2.3. *Wadden coast*

The Wadden coast consists of barrier islands, separated by tidal inlets and their associated ETDs (Fig. 3). In contrast with the Delta area, these ETDs do not interconnect. The ETDs have low-gradient tops (slopes of less than 1:1000) that are dissected by ebb- and flood-tidal channels and have inter-to supratidal sand bars on top. The gradients of the seaward slopes of the ETDs are ranging from 1:1000 to steeper than 1:100 at their most seaward part. The shoreface slopes down to the −20m contour with gradients between 1:100 and 1:1000 and has a width of 8.7–12.5 km. Smaller-scale morphological elements, such as isolated shore-oblique sand bars, reef-bow or saw-tooth bars at the downdrift sides of the ETDs offshore of Terschelling, Ameland and Schiermonnikoog, and elongated coast-parallel breaker bars, have been identified. Offshore Vlieland, a sand ridge and a plateau with an escarpment on its seaward side occur within the lower shoreface. To the northwest of Ameland Inlet, the 20m depth contour shows a lobe-like seaward extension (which has been interpreted to be an older ETD of Ameland Inlet by Sha, 1989b). The shoreface grades to the east into the mouth of the Ems estuary and the comparatively small ETDs of the inlet channels east of Schiermonnikoog. Sand waves occur in all areas.

### 2.2.4. *Ebb-tidal deltas*

Ebb-tidal deltas constitute the shoreface at the seaward side of tidal inlets. The morphology of an ETD is essentially determined by the balance of wave- and tidal energy. Wave-dominated ETDs are pushed close to the inlet throat, while tide-dominated ETDs extend offshore. See Elias et al. (2017) for an extensive summary of the relevant literature on ETD morphodynamics. The main channels in tidal inlets along the Dutch coast are ebb-dominated. They build terminal lobes that can expand seaward due to sediment supply and deposition. The down-drift side of the ETDs is shallow, since large channels are absent. These shallow sand masses, mostly dominated by waves, are usually separated from the adjacent island coast by a flood-dominant shortcut channel.

Most ETDs along the Dutch coast have been impacted by interventions in tidal basins such as partial or complete damming. These impacts include (i) erosion of the seaward edge of the ETD by waves down to c. −10 m, part of the eroded sand is stored in intertidal sand bars, (ii) a relative increase of the shore-parallel North Sea tidal currents which causes local changes in channel orientation, and (iii) flattening out of intertidal bars and infilling of the now oversized channels with sand and (imported) mud. For examples and details from the Delta area and the Friesche Zeegat, see, respectively, Elias et al. (2017), van der Spek and Elias (2021) and Oost (1995), Elias and Oost (2021). Moreover, changing phase differences between inlet tide and North Sea tide affect the orientation of the main channels. The reduction in phase difference (without a significant change in tidal volume) in Texel and Vlie Inlet due to construction of the Afsluitdijk caused the main channels to rotate in updrift direction, diminishing the influence of the tidal flow in the shallow ETD platform and exposing it to increased wave attack. See Elias and van der Spek (2006; 2017) for details on the changes in the ETD of Texel Inlet.

#### *2.2.5. Shoreface-connected ridges*

Along the central part of the Holland coast a series of shoreface-connected ridges of 1–6 m height occurs (Fig. 3). Van de Meene (1994) studied them extensively, he ran bathymetric transects over the ridges, and collected box cores for analysis of sediment grain sizes and sedimentary structures. Moreover, he constructed side-scan sonar mosaics to reveal the sea-bed morphology. The mosaics showed straight-crested sand waves with superimposed straight-to sinuously crested megaripples on top of the ridges.

In addition, Van de Meene ran a seismic survey across the ridges and collected a set of closely spaced vibrocores along the seismic lines. The seismic sections showed signatures of infilling and migrating tidal channels, confirmed by the deposits in the vibrocores. On top of this, fine-to medium-grained sand containing an open-marine *Spisula* fauna occurred. Van de Meene concluded that the ridges are composed of marine sand (with exception of the most southern part), and that they are gradually building out to the northwest with time.

The most southern seismic transect shows that in that part, the ridge topography has been carved out in older sediments, which indicates that the ridge morphology there is more an erosive feature than a depositional phenomenon, as it is along the seismic transects farther north. Moreover, he concluded that the ridges are still active in the present hydrodynamic regime and that they are migrating seawards very slowly.

### *2.3. Shoreface sediments and bedforms*

The seabed at the shoreface is predominantly sandy, with some clay deposits, and an admixture of gravel and shells. South of Alkmaar, the mobile sea-bed layer consists of reworked Pleistocene and older Holocene deposits and includes alluvial sand of the rivers Rhine and Meuse. Median grain sizes range from 250 to 300 μm. North of Alkmaar the seabed consists of reworked (peri-)glacial sands from the Pleistocene. Along the Wadden coast the median grain size fines to the east, from 210 to 300 μm offshore Texel to 63–150 μm offshore Schiermonnikoog (Niessen, 1990). Reworking of glacial tills near Texel and Vlieland produced gravel-rich lags (see Sha et al., 1996). Large tidal channels near tidal inlets cut into the seabed and excavate Pleistocene (Wadden area) and (pre-)Quaternary deposits (Delta area), see Sha (1989a) and Ebbing and Laban (1996) and van der Spek (1997) respectively. Hijma (2017) presents a comprehensive overview of both the shoreface geology and the impact of erosion-resistant layers on tidal-channel migration.

The grain-size distribution of the sand on the shoreface is variable over time and reflects the variation in driving forces. Passchier and Kleinhans (2005) described median grain sizes (250–350 μm) and the variation in small-scale seabed morphology of the central Holland shoreface at 14–18 m depth over a one-year period. They found two-dimensional megaripples in areas dominated by tidal currents and 3-D megaripples where wave influence increased. After storms they noticed undulating bed topography covered with smaller 3-D megaripples. Guillén and Hoekstra (1996) reported that at Terschelling comparatively coarse nourishment sand was quickly redistributed over the (upper) shoreface to restore the equilibrium distribution of grain-size fractions in response to average hydrodynamic conditions. Van Straaten (1965) and van der Valk (1996) reported medium-grained sand ($D_{50} > 260$ μm) at the shoreface below 12 m depth, overlain by a zone of fine-grained sand ($D_{50} \leq 150$ μm) with a coarsening-upward surfzone and beach sequence ($D_{50} \geq 210$ μm) on top of mid- and late Holocene shoreface deposits in the prograded barrier sequence of the Holland coast. Van de Meene (1994) found a comparable change from medium-grained brown sand ($D_{50} = 250$–$300$ μm) at the inner-shelf and lower shoreface towards fine-grained grey sands ($D_{50} = 150$–$200$ μm) higher up at the shoreface at a depth of 10 m. However, this was not confirmed for all locations in the present-day situation (Niessen and Laban, 1987).

### *2.4. Observations on large-scale shoreface morphodynamics*

To establish the large-scale morphodynamic changes at the shoreface, the North Sea Directorate of Rijkswaterstaat used dredged sand to build sand bodies on the shoreface and monitored their evolution. Van Woudenberg (1996) described the development of a shore-normal sand dam that was built near Hook of Holland in 1981–1982, at depths of 15–23 m. The dam with an initial trapezoidal shape was 3600 m long, 250–370 m wide at its base and 1.3–4.1 m high. The part of the dam deeper than −19 m did not migrate over the period 1982–1995. However, this part of the dam declined slightly in height and transformed into an asymmetrical, peaked profile with a gently sloping southside and a steep northern side (resembling the profile of offshore sand waves). Moreover, the dam was covered with megaripples (height 0.2–0.5 m, length 10 m). The upper part of the dam, shallower than −19 m, was not stable over the interval 1982–1995. This part migrated up to 150 m to the northeast and lost height. A distinct asymmetry did not develop, possibly because of wave activity. Van Woudenberg concluded that the depth of transition from the stable to unstable part of the dam at −19 m coincided with the lower boundary of the active coastal profile.

Verhagen and Wiersma (1991) analysed the development of a sand mound slightly north of IJmuiden. The sand was dumped on the sea bed between −10 and −15 m and had a maximum height of 1.2 m. Based on depth soundings they observed that the mound migrated to the northeast over the period 1982–1990 and that the migration rate was larger in the shallow parts than in the deeper parts. They concluded that the migration was caused by daily wave and current conditions and not by extreme events. Cross-shore sediment transport, either landward or seaward, could not be established.

Van Heteren et al. (2003) monitored 2 sites at the central Holland shoreface from March 2001 until April 2002, using a multibeam echo sounder, a side-scan sonar and a boxcorer. One site was situated on the margin of an area of sand waves on a shoreface-connected ridge (Fig. 4), the other at the transition of the lower shoreface to shoreface-connected ridges. For both areas 4 successive multibeam bathymetries were collected. Passchier and Kleinhans (2005) analysed the data and concluded that two-dimensional megaripples are the dominant bedform in current-dominated tidal flow regimes with minor wave influence. With increasing energy conditions 3-D megaripples start to form and during storms an undulating bed topography of mound-like 3-D

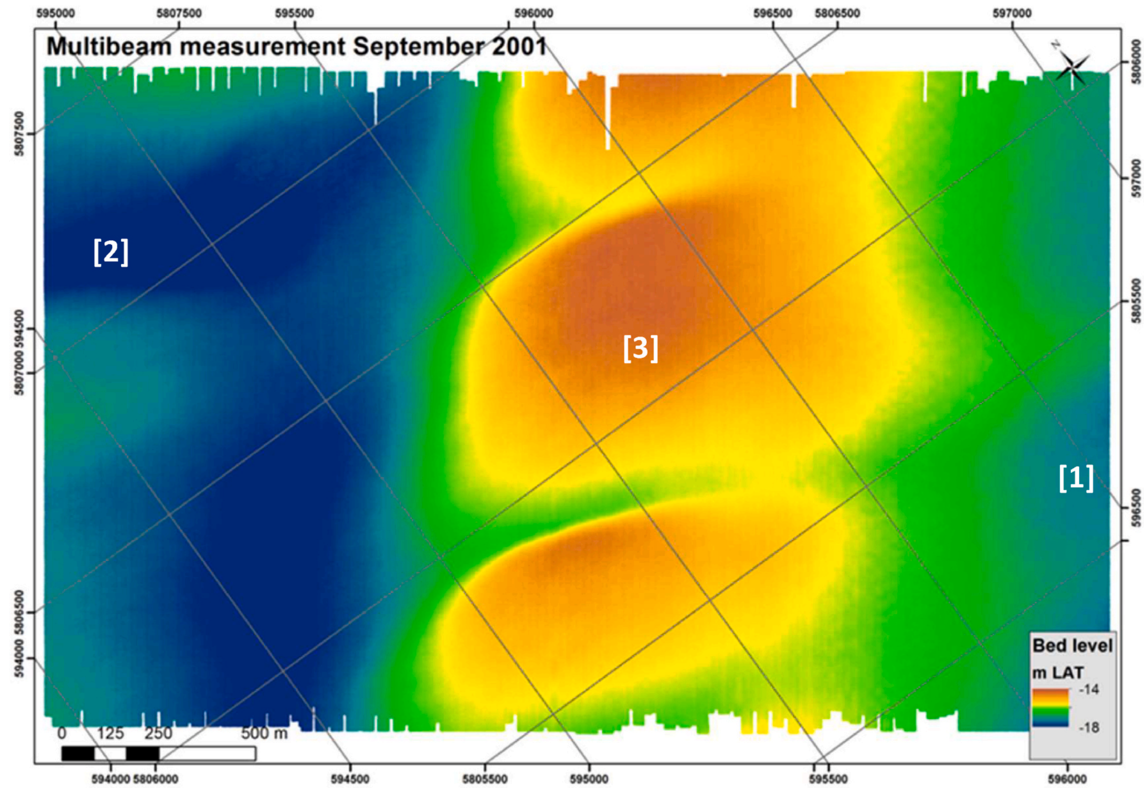


**Fig. 4.** Multibeam sonar image of a shoreface-connected ridge with sandwaves on top, located 5–10 km offshore and about 10 km south of IJmuiden. Landward is to the right. On the landward side, the area is dominated by a flat seafloor without major bedforms and a slope of less than 1:1000 [1]. On its seaward side, the area is characterised by sand waves that are 2–4 m in height and that have wavelengths of tens to hundreds of meters [2]. A shoreface-connected ridge covered with sand waves on its seaward side occurs in the central part of the area [3]. Coordinates are in UTM.

bedforms develops. The variable size of the megaripples over time indicates that the shoreface is a dynamic environment, sensitive to strong wind conditions. During (minor) storm conditions the areas influenced by wave activity expanded in the direction of the inner shelf and beam-trawl tracks were largely obliterated. See Passchier and Kleinhans (2005) for more details.

Analysis of depth changes at the shoreface of the Holland coast below the surf zone (Vermaas, 2010; Vermaas et al., 2015) reveals that vertical variation around time-averaged coastal profiles decreases with depth until a minimum is reached. Farther seawards the range of variation is constant. The depth of this point of minimal vertical variation increases from south to north from −11 m in the Delta area to −15 m along the Holland coast. Along the Wadden coast it decreases from −13 m at Texel to −10 m at Ameland. Moreover, the profiles did not show a measurable offshore sediment transport, despite the addition of large volumes of sand to the upper shoreface in many locations. The data set of yearly profile surveys that started in 1965, the so-called Jarkus data, shows that the lower shoreface of parts of the Holland coast has lowered with up to 1 m.

### 2.5. Shoreface sand transport processes

Sand transport on the lower shoreface is episodic, determined by high-wave events, and typically bedload-dominated. Except following storm events, current- (mainly tide) and wave-induced small-scale bedforms with typical heights of 0.02–0.04 m and lengths of 0.4–0.6 m were frequently observed on the lower shoreface. Also, the observed variation in grain-size distributions with time at the lower shoreface reflects the impact of varying wind and wave conditions. Typical estimates of the annual net cross-shore transport rates at the 20m depth contour are 0–20 $m^3$/m/year in the onshore direction (van der Werf et al., 2017), which amount to 0–2 million $m^3$/year into the Holland coast area. At the 8m depth contour on- and offshore-directed transport processes seem to cancel each other out, leading to a nearly zero net cross-shore transport from the lower to the upper shoreface along the Holland coast (van Rijn, 1997). It is unclear what typical net transport rates are in between 20 m and 8 m water depth. The episodic nature, relatively low values and the important bedload contribution make it very difficult to accurately measure and predict lower shoreface sand transport processes. In addition to that, the sediment composition of the inner shelf of the North Sea is not really different from that of the active shoreface sand, which precludes the tracing of shoreface sand transported offshore during storm events.

The generally and internationally accepted conceptual model for cross-shore sediment transport on the shoreface comprises a short-term circulation of sand, including bar morphodynamics, on the upper shoreface and a much slower, long-term circulation on the lower shoreface. Upper shoreface dynamics are driven by daily wave processes whereas at the lower shoreface sand is transported offshore during storms by downwelling currents that bring the sediment out of reach of the daily wave processes, followed by a slow return of this sand volume driven by more energetic wave conditions (see, e.g., Cowell et al., 2003, Hamon-Kerivel et al., 2020; Anthony and Aagaard, 2020). Aigner (1985) described storm beds that are deposited on the North Sea floor offshore the German Wadden islands that are supposed to have formed by storm-driven downwelling currents. These beds grade from dm-thick laminated sandy sequences with reworked shells at their base and a mud layer on top at the shoreface, into mm-thin laminated sands and silts offshore. The latter kind of deposit has not been found offshore the Dutch coast. Agaard (2011) determined the sediment budget for part of the Danish North Sea coast combining cross-shore profile analysis, numerical modelling and field measurements of cross- and longshore sediment transport at the boundary between upper and lower shoreface. He concluded that a substantial part of the longshore sediment supply by wave-driven currents is transferred seaward across the shoreface by systematically offshore-migrating nearshore bars that deliver sediment to the lower shoreface. In a later paper, Agaard (2014) used measurements of suspended sediment load and cross-shore transport on the lower shoreface at five different field sites that exhibit a wide range of wave conditions (from short-period wind waves to swell) and sediment characteristics, to put together a model for sediment supply from the lower to the upper shoreface at large spatial and temporal scales. The applicability of both the concept of seaward sediment transport by offshore migrating bars and the long-term cross-shore sediment exchange model for the Dutch coast needs to be assessed.

## 3. Methods

### 3.1. Study areas

Between and within the Delta, Holland and Wadden coast there are large differences in the dominant hydrodynamic processes, morphodynamics and human interventions. To address these differences, three study areas with contrasting settings were selected. The study areas Noordwijk, Terschelling and Ameland Inlet (Fig. 5) represent contrasting settings: the continuous Holland coast vs. the segmented Wadden coast (Noordwijk – Terschelling) and barrier-island lower shoreface vs. the lower shoreface of an ebb-tidal delta (Terschelling – Ameland Inlet). Importantly, the Ameland Inlet study area forms the seaward extension of the study area of the Kustgenese 2.0 Tidal Inlet project and the SEAWAD research project that was funded by the Dutch Research Council NWO. The shores of the former islands of the Delta area are bounded by the channels of the adjacent ebb-tidal deltas. They are dominated by tidal flow, the wave-current interaction typical for the lower shoreface is likely to be small or absent. Therefore, no study area was chosen here.

#### 3.1.1. Ameland Inlet

Ameland Inlet is located between the barrier islands Terschelling and Ameland. It is one of the most intensively investigated inlets in the Dutch Wadden Sea and it is the main subject of study of the Kustgenese 2.0 Tidal Inlet project and the affiliated NWO SEAWAD research project (see e.g. van Prooijen et al., 2020; Elias et al., 2022, this issue). The study area extends to the most seaward part of the ebb-shield, the shallow area


**Fig. 5.** Location of the study areas of the Kustgenese 2.0 Lower Shoreface project along the Dutch coast. See Fig. 1 for orientation.

at the end of the main ebb channel (Fig. 6a), in order to extend the measurements in the inlet and ebb-tidal delta in seaward direction. The ebb-shield has a steep seaward slope, decreasing from −6 m to −19 m in about 1 km (Fig. 6b). The study area measures c. 5 km × 4 km.

### *3.1.2. Terschelling*

The study area at Terschelling is located in front of the middle of the island (Fig. 7a). This part of the island forms a wave-dominated, uninterrupted coast and is also outside the direct influence of the tidal inlets Vlie Inlet in the west and Ameland Inlet to the east. The upper shoreface shows breaker bars, at the lower shoreface megaripples can be expected. The slope of the profile does not decrease around −15 m, but remains almost constant up to −20 m, where it becomes more gradual (Fig. 7b). The study area measures c. 6 km × 6 km.

### *3.1.3. Noordwijk*

Noordwijk is located at the uniform, straight, Holland coast, about 35 km north of Hook of Holland. The coastline has an orientation of approximately 28° clockwise to the north (Fig. 8a). At the upper shoreface breaker bars are present and the steep slope is uniform down to a depth of c. −15 m. In seaward direction, the gradient decreases to c. 6 km distance where ridges occur (Fig. 8b; note that the landward ridge is not shoreface-connected). On their seaward side, the ridges merge into a field of shore-normal sand waves (that does not show up on the profile). The area measures c. 13 km × 5 km, its depth ranges between −8 m and −20 m, which excludes the sand bars of the surf zone.

## *3.2. Data collection surveys*

The study areas were sampled between July 2017 and October 2018 (Table 1); vibrocores were collected in July 2017, box cores in July 2017

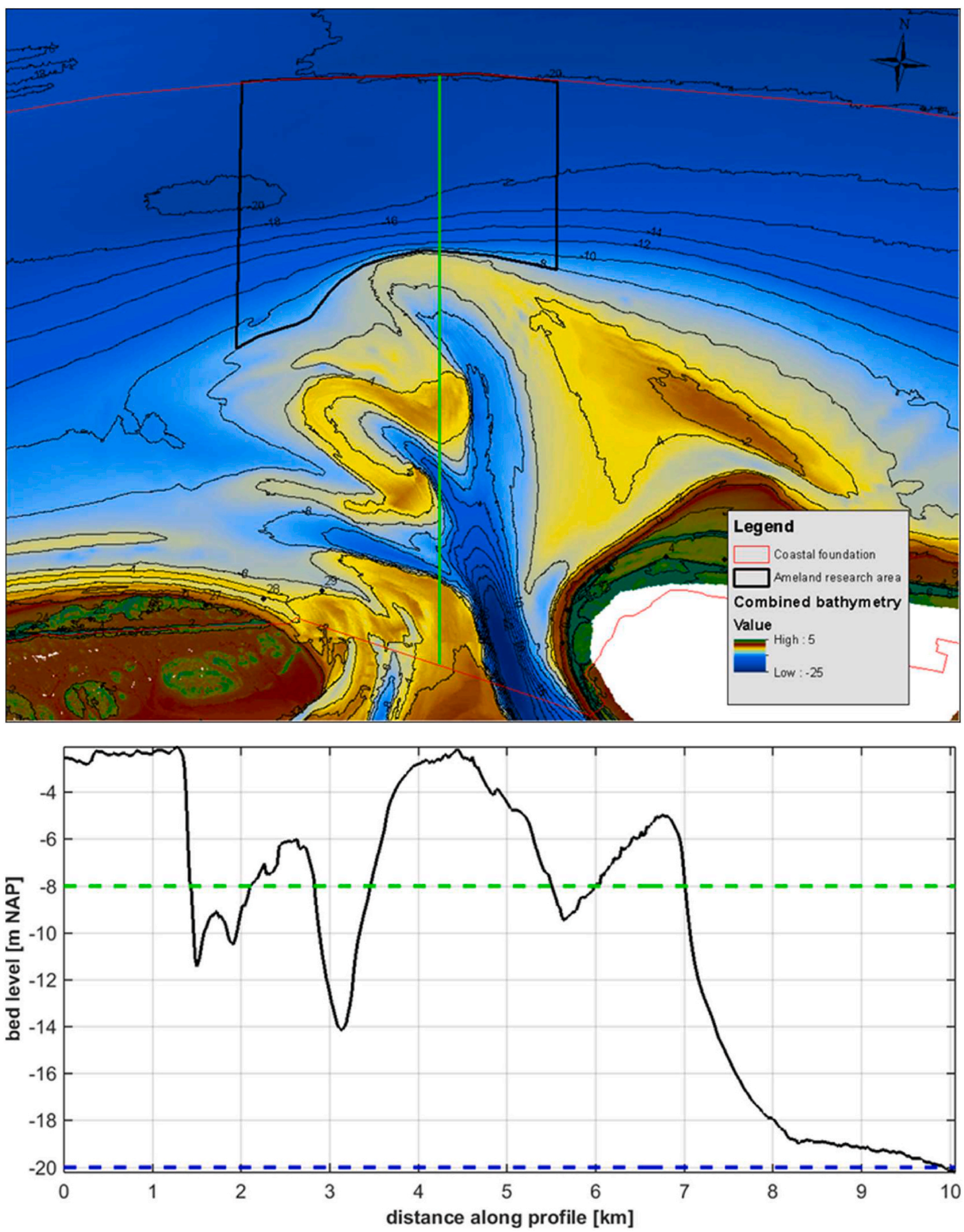


**Fig. 6.** (a) Bathymetry/topography of Ameland Inlet and its ebb-tidal delta. The black lines indicate the study area, the red line indicates the seaward boundary of the coastal foundation and the green line indicates the location of the profile (map is rotated, see north arrow; bathymetry based on depth soundings over the years 2009–2014); (b) shoreface profile at study area Ameland Inlet, the green dashed line is NAP -8m, the blue dashed line is NAP -20m.

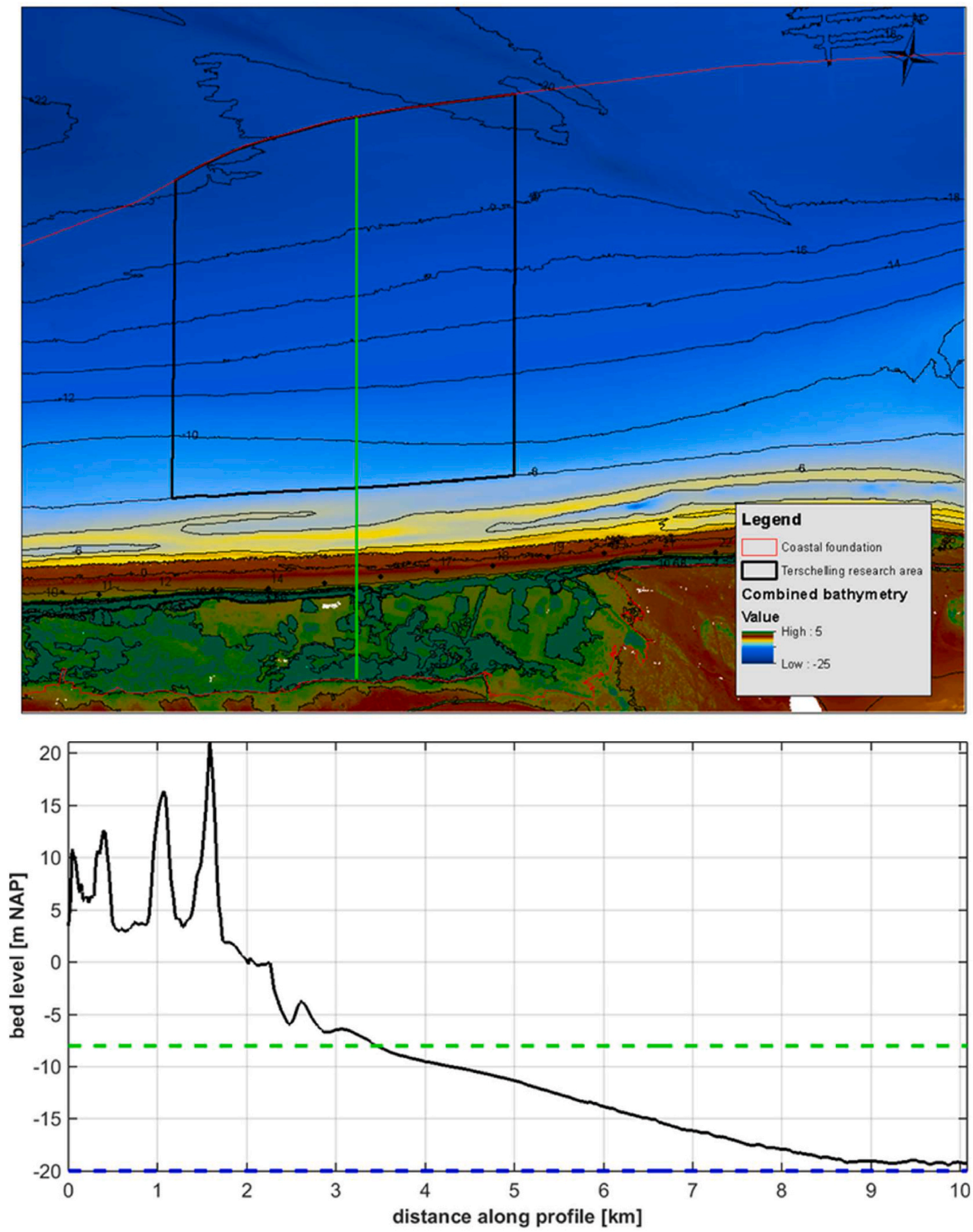


**Fig. 7.** (a) Bathymetry/topography of the central part of Terschelling. The black lines indicate the study area, the red line indicates the seaward boundary of the coastal foundation and the green line indicates location of the profile (map is rotated, see north arrow; bathymetry based on depth soundings over the years 2009–2014); (b) shoreface profile at Terschelling study area, the green dashed line is NAP -8m, the blue dashed line is NAP -20m.

and October 2018. Multibeam echo sounding was carried out in two intervals, September to December 2017 and August to October 2018 (Tables 1 and 2). Measuring frames were deployed four times in total between November 2017 and May 2018. See van Prooijen et al. (2020) for an overview of the data collected in the Ameland Inlet area and van der Werf et al. (2019) for the other areas.

### 3.2.1. *Multibeam echosounding*

To get detailed information and complete areal coverage of bathymetry and bedforms, the study areas were surveyed using an EM2040c Dual Head hull-mounted multibeam echosounder in the autumns of 2017 and 2018. The multibeam echosounder swaths were sailed parallel to the shoreline to avoid offset by the shore-parallel tidal currents and with 100% overlap. The raw data was processed into a point cloud that was interpolated using inverse-distance weight interpolation to a 0.5m-resolution grid. The resulting high-resolution grids were visualized using ArcMap software. Varying meteorological conditions preceding and during the surveys caused different smaller-scale morphological phenomena. See Oost et al. (2019b) for more details of the multibeam surveys.

### 3.2.2. *Box coring*

Shoreface sediments were sampled with box corers for analysis of sedimentary structures and grain-size distributions. In 2017, 42 stations arranged in transects normal to the coastline were cored with a cylindrical 'box' (Table 3). These boxes do not allow for in-situ sediment observations. Hence, each core was sampled by pushing 3 pvc tubes (0.1 m diameter) into the sediment. The quality of these sub-cores turned out to be poor, no information on sedimentary structures could be retrieved.

In 2018, a new series of 48 closely spaced box cores was collected along one (Terschelling, Noordwijk) or two (Ameland Inlet) coast-normal transects (Table 3). Additional stations were chosen on the

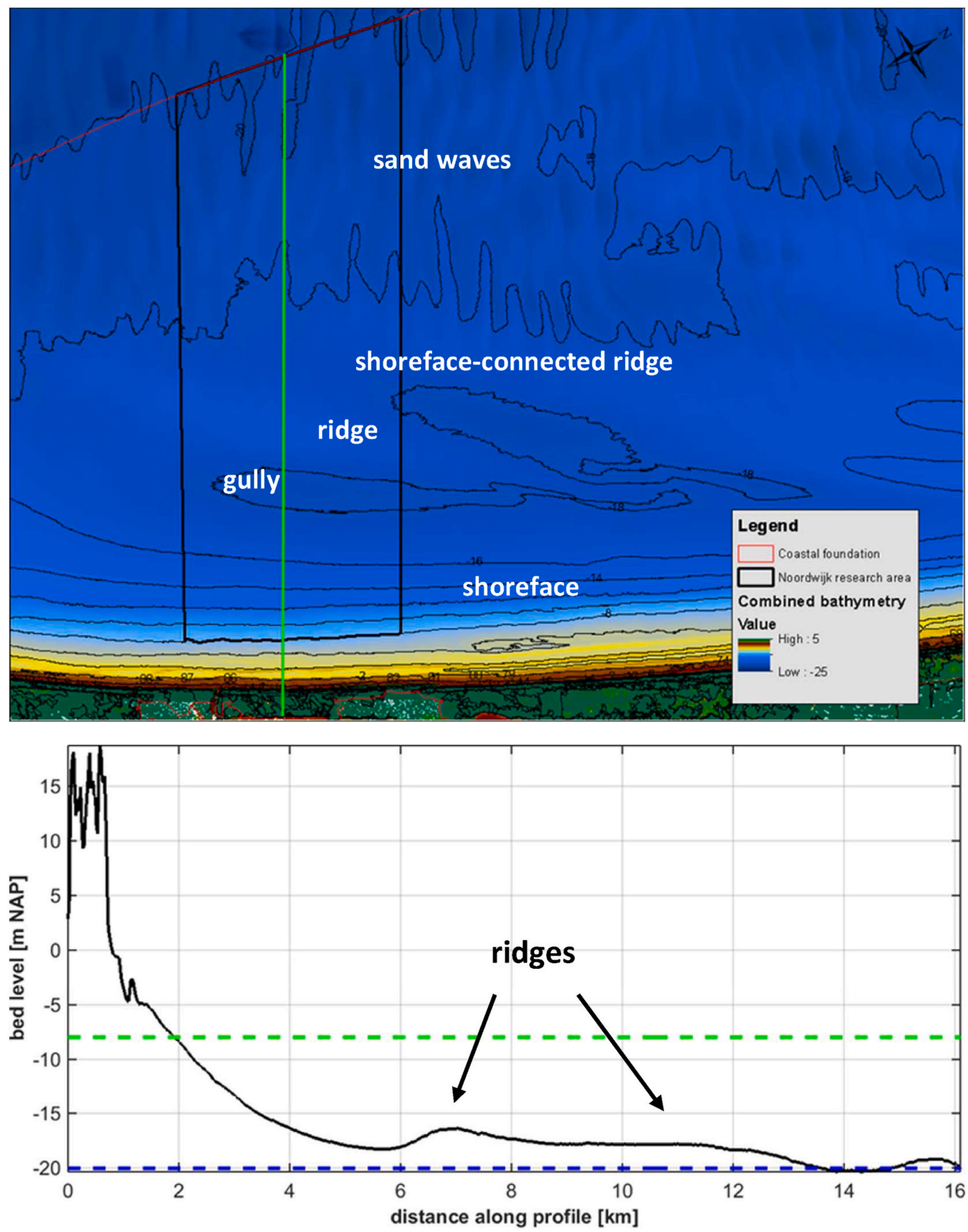


**Fig. 8.** (a) Bathymetry/topography of the coast near Noordwijk. The black lines indicate the study area, the red line indicates the seaward boundary of the coastal foundation and the green line indicates the location of the profile (map is rotated, see north arrow; bathymetry based on depth soundings over the years 2009–2014); (b) shoreface profile at Noordwijk study area, the green dashed line is NAP -8m, the blue dashed line is NAP -20m.

**Table 1**
Overview of the sampling, surveying and frame deployment in the study areas during 2017 and 2018.

| | 2017 | | | | | | | 2018 | | | | | | | | | | | |
|---|---|---|---|---|---|---|---|---|---|---|---|---|---|---|---|---|---|---|---|
| | June | July | Aug | Sep | Oct | Nov | Dec | Jan | Feb | Mar | Apr | May | June | July | Aug | Sep | Oct | Nov | Dec |
| Cores | | vibro/box | | | | | | | | | | | | | | box | | | |
| Multibeam | | | | Ameland | | Terschelling | | | | | | | | | Ameland | Noordw | Terschel | | |
| | | | | | Noordwijk | | | | | | | | | | | | | | |
| Frames | | | | | | Ameland | | Terschelling 1 | | Tersch. 2 | Noordwijk | | | | | | | | |

basis of the 2017 multibeam bathymetry. These stations were sampled using rectangular boxes with a detachable side. The retrieved sediment is shown after removal of the side plate and can be studied, photographed and lacquered. Lacquer peels are casts of the sediment surface that enable the study of sedimentary structures in detail. In total 33 box cores were lacquered.

**Table 2**
Multibeam echosounding intervals of the study areas in 2017 and 2018.

| Study area | 2017 survey | 2018 survey |
|---|---|---|
| Ameland Inlet | 5–7 September | 7–8 August |
| Noordwijk | 21, 25, 26 September<br>19, 20, 23, 24 October<br>13-16, 20–23 November | 13–28 September |
| Terschelling | 28–30 November<br>12 December | 9–12 October |

**Table 3**
Overview of sampling dates and number of box cores per study area.

| Study area | 2017 survey | | 2018 survey | |
|---|---|---|---|---|
| | Sampling date | Number of cores | Sampling date | Number of cores |
| Noordwijk | 3 July | 12 | 6 September | 16 |
| Ameland Inlet | 4 July | 14 | 5 September | 16 |
| Terschelling | 5 July | 16 | 4 September | 16 |

Grain-size distributions were determined for surface samples of the 2017 and 2018 box cores using a Malvern laser-diffraction particle sizer. See Oost et al. (2019a) for more information on box cores and grain sizes.

#### 3.2.3. Vibrocoring

To further detail insights into the composition and distribution of Holocene and late Pleistocene deposits at the surface and in the shallow subsurface of the lower shoreface of the Dutch coast, a series of 23 vibrocores was collected along 8 transects normal to the coastline in the study areas (Table 4), using a hydraulic vibrocorer. The weather during coring was calm. The sediments were collected in a 10 cm diameter pvc liner tube within a 6 m long core barrel driven by three-ton weight and a vibrator motor. The vibrocores had a maximum length of 5.5 m (with a minimum length of 2.45 m and an average of 4.24 m) and were cut in 1-m-long pieces, drained, capped and stored vertically. Subsequently, the vibrocores were transported to the Deltares facilities, where they were opened, photographed and described. Grain sizes were visually estimated using a binocular microscope and a sand ruler. The sediments in the cores were classified in sedimentary facies, based on lithology, sedimentary structures, and shell content. Finally, the sedimentary facies that were interpreted as depositional environments. See Van der Spek et al. (2022; this issue) for more details.

#### 3.2.4. Process measurements

Physical parameters such as current velocities, sediment concentrations and ripple dynamics were measured at and just above the seabed. Custom-made frames were equipped with Acoustic Doppler Velocimeters (ADVs) and upward- and downward-looking Acoustic Doppler Current Profilers (ADCPs) to measure current velocities, Optical Backscatter sensors (OBS) and a LISST laser in-situ scatter and transmission sensor to measure sediment concentrations, a 3D SONAR to register (migrating) small-scale bedforms and a Multi-Parameter Probe that can be used to calculate salinity and density, and to analyse the interaction between physical and biogeochemical processes. The ADV and ADCP instruments incorporated pressure sensors that register variations in water level. The frames were deployed on transects approximately perpendicular to the coast at two or three different water depths (Table 5). The deployment period varied between 2 and 6 weeks. More information on the instruments and measurements can be found in van der Werf et al. (2019) and van Prooijen et al. (2020). Van der Werf et al. (2022; this issue) describe the data processing. For more information on KG2 field observations, see van der Werf et al. (2019) and Schrijvershof et al. (2019).

**Table 4**
Information on the collection of vibrocores from the study areas.

| Study area | Number of cores | Sampling date |
|---|---|---|
| Noordwijk | 8 | 3 July 2017 |
| Ameland Inlet | 9 | 4 July 2017 |
| Terschelling | 6 | 4–5 July 2017 |

### 3.3. Modelling

Sand transports in the DLSF were calculated with a tailor-made numerical modelling approach. A three-dimensional Delft3D flexible-mesh model of the North Sea was used to calculate tide-, wind- and density-gradient driven currents with real-time forcing over the years 2013–2017. Flow was calculated independently of waves. The model covers the complete DLSF, however with a relatively low resolution of 900 m. Nearshore wave data were obtained using a wave-transformation matrix based on offshore observations. The calculated waves and currents were validated against KG2 and earlier data. The model performs generally well, but its performance decreases with decreasing water depths, indicating the increasing importance of wave-induced flow (Grasmeijer et al., 2019). Moreover, the model underpredicts the currents under high-wave conditions.

A one-dimensional, velocity averaged Van Rijn 2007 sand transport model was deployed to calculate the sand transport on the 20m depth contour ($D_{50}$ = 250 μm; incl. pores). Return flow was not included which overestimated the cross-shore transport by 11–18%. For detailed information on the modelling, see (Grasmeijer et al., 2019; 2022, this issue).

## 4. Results and interpretation

This section gives an overview of the project results, based on the interpretation of collected data and modelling.

### 4.1. Shoreface deposits

Six different depositional environments were distinguished: active layer, seabed deposits, lower-shoreface deposits, ebb-delta channel deposits, tidal channel deposits, and alluvial (river) channel deposits. The several dm-thick active layer forms the mobile top of the seabed-, lower-shoreface- and ebb-delta channel deposits. Ebb-delta channel deposits (probably grading into terminal-lobe deposits) are restricted to the Terschelling and Ameland Inlet areas, fluvial deposits to the Noordwijk site. See Van der Spek et al. (2022, this issue) for full details.

Seabed sediment is the product of reworking of underlying deposits, enriched with sediments that have been transported to the location and shells of locally occurring benthic fauna. The *active layer* represents the youngest phase of reworking. It occurs at the top of all cores; it is bright yellow to brown in colour and has a sharp base. The active layers at Noordwijk are richer in shells than at Ameland Inlet and Terschelling. At the Wadden locations *Donax* is the most abundant species, at Noordwijk *Spisula* dominates. *Seabed deposits* at the inner shelf are comparable to active layer deposits, there is a distinction in colour. Seabed sediment at Ameland Inlet is brown-grey to dark grey and fine-grained, its shell content is low and consists mainly of equal amounts of *Donax* and

**Table 5**
Overview of the measurement campaigns in the study areas. Note that a second campaign was run at Terschelling, the wind and wave conditions were too mild to have sufficient seabed dynamics during the first campaign.

| Campaign | Period | Number of frames | Depths (m) |
|---|---|---|---|
| Ameland Inlet | 2017; Nov 8 - Dec 11 | 3 | 10; 16; 20 |
| Terschelling 1 | 2018; Jan 11 - Feb 6 | 2 | 14; 20 |
| Terschelling 2 | 2018; March 12–26 | 3 | 10; 14; 20 |
| Noordwijk | 2018; Apr 4 - May 15 | 2 | 12; 20 |

*Spisula*. At Noordwijk the seabed deposits consist of fine to medium (brown-) grey sand with local silt- or clay layers or some fine gravel at its base. They contain a moderate volume of mostly *Spisula* shells.

*Lower-shoreface deposits* were found at Noordwijk. They consist of parallel- and cross-laminated fine-grained sand, varying in colour between grey and brown. The shell content of these deposits is in general very low. The upper part of the shoreface deposits is reworked, they are slightly coarser in grainsize and abundant in clay layers, especially at the top. Their shell content differs from the overlying active layer; the abundant *Macoma* shells are missing, *Cerastoderma* shells occur instead. This is in contrast with the underlying significantly finer, well-sorted and cross-laminated shoreface sand of the prograded beach barrier of Subboreal age. Both the front of the ebb-tidal delta of Ameland Inlet and the shoreface of Terschelling consist of *ebb-delta channel deposits*. They consist of fine sand with varying numbers of mm-to cm-thick clay layers, shells are very sparse. Type-1 deposits consist of grey, predominantly fine sand with (vague) cross-lamination and abundant clay layers and thin detritus layers. Type-2 deposits consist of (brown-) grey, cross-laminated fine sand with thin layers of clay and locally silty clay (loam), clay flasers, and scattered small peat lumps and thin bands of detritus. In Type-2 deposits the number of clay layers is much lower, they are moreover thinner, and in some cores completely absent. Type-2 deposits always occur above Type-1 deposits, together they form a sequence with an upward decreasing number of clay layers.

*Tidal channel deposits* consist of brown-grey and grey sand with mm-to cm-thick clay layers and local shell layers, peat clasts and organic detritus. Typical are the shells from tidal basin species such as *Cerastoderma*, *Macoma* and *Mytilus*, often mixed with coastal species such as *Spisula*. The base of these deposits is usually sharp. In the Wadden area the sand is predominantly medium grained with short intervals of fine sand, and is abundant in shells of *Cerastodema*, followed by *Mytilus*. Along the Holland coast, the sand is predominantly fine-grained, the shell content is low, *Macoma* is the dominant species, followed by *Mytilus*. These deposits formed during the lateral migration and/or infilling of tidal channels. *Fluvial deposits* consist of brown-grey to red cross-laminated sand without shells. These deposits were formed by Pleistocene braided rivers.

The front of the ebb-tidal delta of Ameland Inlet is steep and consists of material supplied by the main ebb channel. These ebb-delta channel deposits are reworked by waves and currents, they grade seawards into seabed deposits. The low-gradient shoreface of the Terschelling site consists of a thin active layer on top of ebb-delta channel deposits. At the Noordwijk site fluvial deposits with incised bodies of tidal channel sand underlie a steep shoreface and a ridge-swale topography farther offshore. The ebb-delta channel deposits at the shoreface of Terschelling are similar to those at the front of the ebb-tidal delta of Ameland Inlet. Moreover, the tidal channel deposits that are common in the Noordwijk area, occur in only one core at Terschelling. This indicates that the deposits underlying the shoreface of Terschelling were formed in the ebb-tidal delta of a precursor of Ameland Inlet and not in the transgressive setting of a retreating barrier island. These deposits were possibly formed as part of the ebb delta of the Middelzee, a large medieval predecessor of the Ameland tidal basin.

Reworking of the shoreface of the prograded Subboreal beach barriers at Noordwijk at water depths of 12.5–13.5 m produced a 1.1-m-thick series of fining-upwards storm beds, including the active layer. At the shoreface of Terschelling storm beds are missing at these depths and only an active layer 0.2 m thick occurs. This suggests that the largest part of reworked sediment at Terschelling is carried off, which implies large-scale erosion of the shoreface.

The stratigraphy of the lower shoreface plays a role in its morphological character and behaviour. Compacted Holocene and Pleistocene clay layers, where not covered by thick sand layers, are likely to show up in the shoreface bathymetry.

### 4.2. Shoreface morphology

The large-scale morphological patterns in the multibeam bathymetries of the study areas that were surveyed in 2017 and 2018 confirm the bathymetries shown in Figs. 6–8. However, on a finer scale the surveys showed interesting details that have not been reported before. Moreover, the repeated surveys did show significant differences in these details that were likely caused by variation in the hydro-meteo conditions preceding and during the surveys. In general, the conditions preceding and during the surveying of the Terschelling and Noordwijk areas were more energetic in 2017 than in 2018.

At the lower shoreface, bedforms created by tidal flow, by wave orbital motions and by their combined effect can be expected. Tidal currents tend to form megaripples that migrate in the direction of the dominant current. Orbital motions caused by waves tend to create shore-parallel bedforms. The combination of tidal flow and wave orbital motions triggers the formation of a different, more three-dimensional ripple type, which may lead to hummocky cross-bedding. For further details on the multibeam surveys and an extensive discussion of the interpretations, the reader is referred to Oost et al. (2019b).

#### 4.2.1. Ameland Inlet

Fig. 9 shows the 2017 bathymetry of the slope of the ebb-tidal delta in front of the main ebb channel Akkepollegat at Ameland Inlet, between c. −9 m and −18 m, and the inner shelf of the North Sea offshore of it. The shelf shows a regular pattern of linear megaripples with their crests oriented in north-south direction (Fig. 10). The megaripples (length ≤10 m; height ≤0.5 m) are formed by the tidal currents and are asymmetrical in the direction of the dominant flood current, which means that their eastern sides are steeper than their western sides. See the Supplementary material for details on the megaripples.

Going landwards, in the direction of the ebb-tidal delta, around −18 m, the ripple pattern becomes more chaotic and less continuous, the ripples become smaller and more three-dimensional (Fig. 10, upper panel, [a] → [b]) and from −16 m upwards the ripples disappear altogether (Fig. 10, upper panel [c]). The transition from regular and two-dimensional to irregular and three-dimensional ripples around −18 m shows the increasing influence of waves on the seabed. The absence of megaripples shallower than −16 m is caused by waves dominating the sand transport at the seabed.

In 2018 the seabed of the Ameland Inlet area was slightly different than the year before: at the shelf the megaripples were less regular and slightly lower (length ≤10 m; height ≤0.3 m) and the ripples disappeared around a depth of 15 m (Fig. 10, lower panel). In the south-eastern part of the study area the transition showed a different pattern (Fig. 11, lower panel [5]): the megaripples become higher, their wavelengths increase and the pattern is interrupted by spots without ripples. The change to a flat bed occurs over a short distance.

These differences in megaripple patterns and dimensions were most likely caused by varying tidal current strength since the grain-size ranges are comparable (2017: $D_{50}$ 165–222 μm; 2018: $D_{50}$ 174–248 μm). The upward shift of the boundary between the rippled and the non-rippled area between the 2017 and 2018 surveys can be contributed to lower-energy wave conditions preceding the 2018 survey. During lower-energy conditions, the lower and shorter waves reach less deep, so the zones of wave domination and combined flow extend less far seawards.

#### 4.2.2. Terschelling

The Terschelling study area shows a gently sloping shoreface which grades into the North Sea inner shelf between −18 m and −20 m (Fig. 12). In 2017, the Terschelling study area was surveyed after a prolonged period of relatively stormy weather with significant wave heights exceeding 6 m. The 2017 bathymetry showed small, locally irregular to hummocky megaripples with their crests oriented NNE-SSW (see Supplementary material).

At the shoreface at approx. −15 m, a distinct gully-like feature occurs

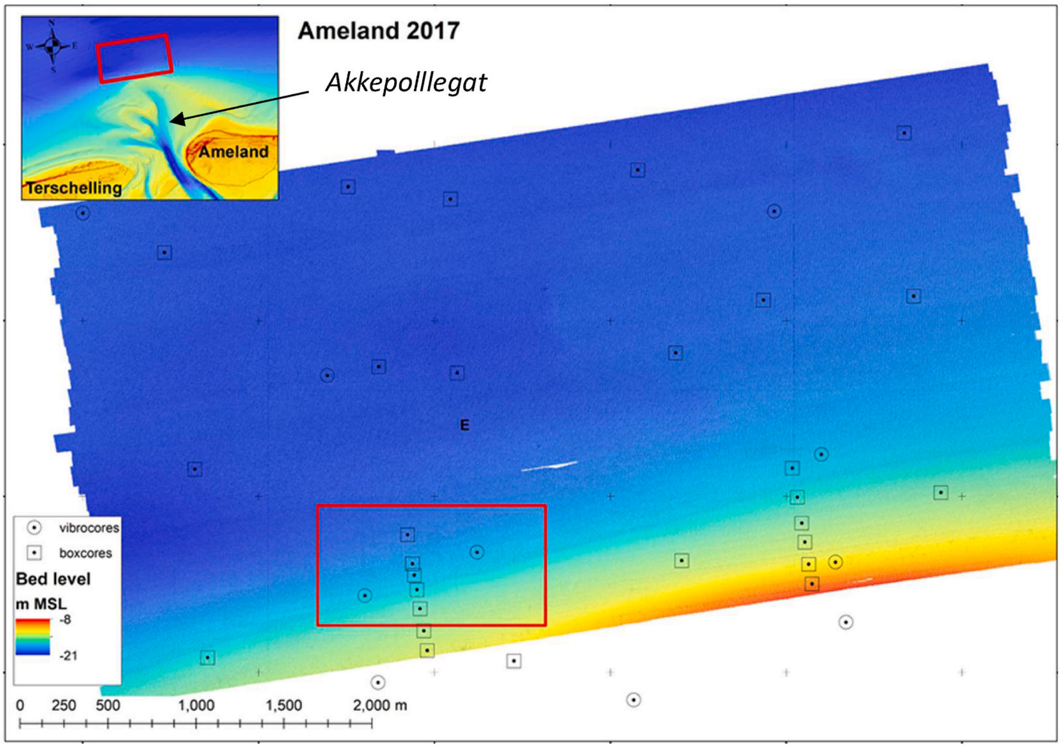


**Fig. 9.** Multibeam bathymetry of the Ameland Inlet study area in 2017, depth ranging between −8 m and −21 m. The positions of vibrocores (circles) and box cores (squares) are indicated. Inset is position of Fig. 10.

that can be traced to the north-west into deeper water (Fig. 13, top panel). The north-eastern side of the gully has a higher elevation than the south-western side. Such a gully-like feature at the shoreface has not been reported before. The persistent nature of the gully (it is still visible in the 2018 survey, see Fig. 13, lower panel) and the higher elevated side to its northeast is probably caused by an erosion-resistant layer in the subsurface. Seismic profiles collected in the north-eastern part of the study area (Sha, 1989b; Sha and de Boer, 1991) show series of stacked channel fills of mid-to late Holocene age that were in part filled in with muddy sediments. It is likely that this gully is scoured into a channel fill and acts as a conduit for seaward flows of water and sediment down the shoreface, e.g. caused by return flows during a high wave event. The vibrocores from the shoreface of Terschelling (see section 4.1 and van der Spek et al., 2022, this issue) do not show shoreward extending clay layers that could have acted as a guiding surface for groundwater, so freshwater outflow at the shoreface resulting in gully formation, is highly unlikely.

In 2018, the seabed of the Terschelling study area showed a similar image as in 2017. Meteorological and wave conditions were calm during the survey and the preceding weeks. Interestingly, the appearance of the aforementioned gully was less prominent than the year before (Fig. 13, lower panel), possibly caused by deposition of sediments in and over it under the calm conditions in 2018. Infilling of the gully with sediment implies (partial) inactivity, viz. reduced or lacking seaward flows. In contrast, the 2018 survey clearly showed 1-m-deep craters in the seabed at the southwestern part of the shoreface at −15 m to −16 m depth (Fig. 14). In 2017 these craters were much smaller and shallower besides smaller in number. The craters are interpreted as pockmarks. Pockmarks are formed by seepage or abrupt expulsion of gasses or fluids escaping from the subsurface. They occur in the Southern Bight of the North Sea (see, e.g., Schroot and Schüttenhelm, 2003; McGinnis et al., 2011; Krämer et al., 2017) but have so far not been reported from the inshore area of the Wadden coast. Since reservoirs of natural gas have been discovered at kilometre-depth underneath the island of Terschelling and the adjacent North Sea, the outflow of gas is the likely cause for pockmark formation. Their clear expression in 2018 likely resulted from the calmer conditions that resulted in low rates of sand transport and hence limited compensation of gas escape.

#### 4.2.3. Noordwijk

The Noordwijk study area comprises several large-scale elements. Going seawards, the shoreface slopes down to −18 m beyond which the seabed rises again to −16 m where crossing sand ridges (see Fig. 8 for overview). Going farther seawards, depth increases slightly to −18 m where crossing the flat top of the shoreface-connected ridge that merges into a field of shore-normal sand waves. An overview of the seabed morphology of the Noordwijk study area is available in the Supplementary material.

In 2017, the Noordwijk area was surveyed during and after a prolonged period of recurring stormy weather. In the weeks preceding and during the survey (21 September - 23 November) 5 events with waves with significant heights of over 4 m from the northwest were registered by the wave buoy Eierlandse Gat, 110 km north of the study area. The shoreface showed a distinct spur-like extension to the southsouthwest (Figs. 15 and 16 [1]). Between the shoreface and the spur, a sinuous erosional path occurred (Fig. 16, top panel [2]). The shoreface showed typical small- and larger-scale depressions besides (0.2–0.4 m deep, tens of meters wide) with various orientations and shapes, especially at its southern half. The top panel of Fig. 16 shows tongue-like depressions [3], the longer ones oriented to the southwest [4]. When the shoreface part of the multibeam data is detrended (by removing the water-depth), it shows the deviations from the average cross-shore profile, and the gullies become more distinct. The detrended data (Fig. 17), clearly show the ‘spur’ [1] and the associated sinuous gully [2], and the tongue-like [3] and southwest oriented depressions [4]. Further north, more gullies parallel to the ‘spur’ [5] and shore-normal features [6] occur along the shoreface between −11 m and −15 m. These features have not been reported before.

Interestingly, megaripples did not occur on the seabed at the toe of the shoreface between −16 m and −18 m, nor in the shore-parallel

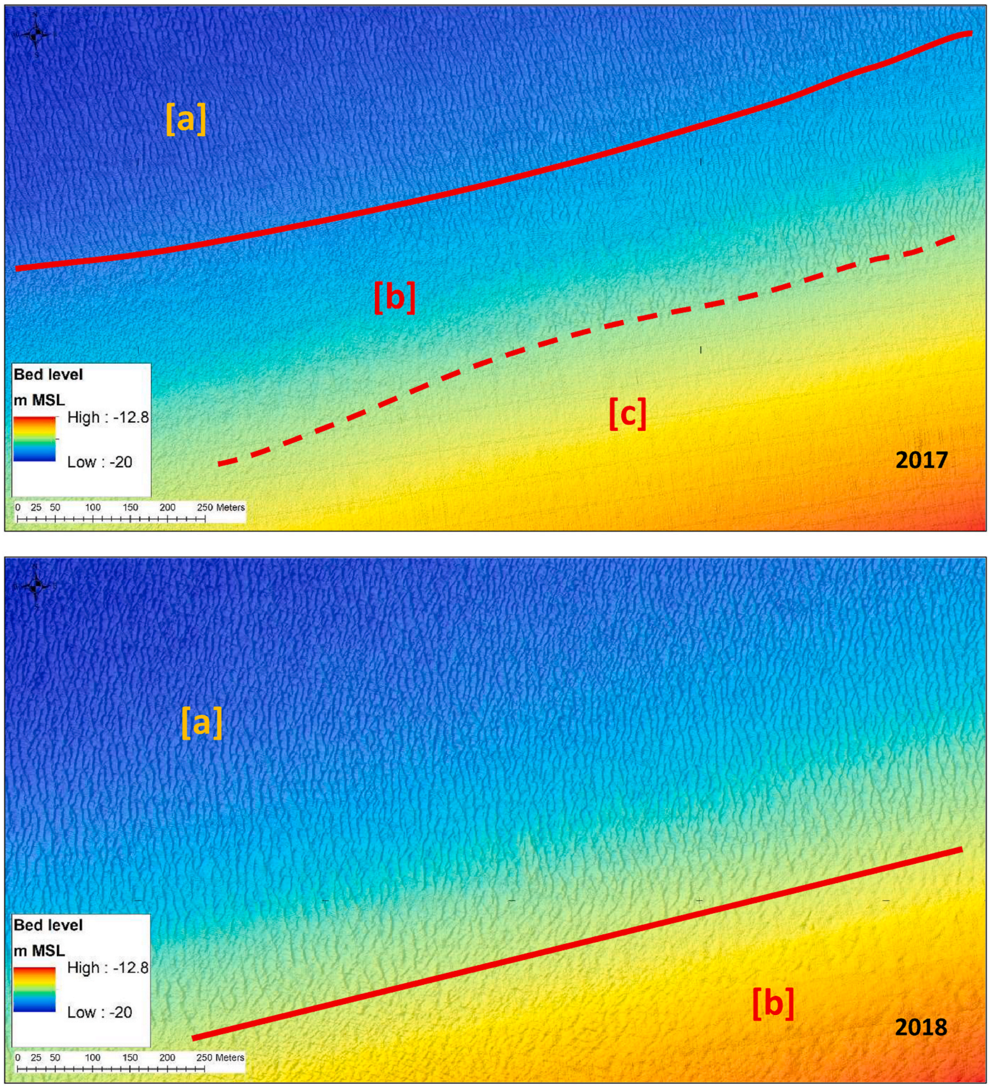


**Fig. 10.** Detail of the Ameland Inlet study area (see Fig. 9 for position), showing the shift in transition from 2D to 3D ripple morphology from 2017 to 2018. The depth of the transition from regular linear megaripples [a] to patchy, irregular 3D ripples [b] and finally a smooth seabed [c] varies with the wave climate. In 2017, the transition occurred at −18 m, in 2018, during a calm period, this occurred shallower (−15 m).

trough between the shoreface and the sand ridge (Fig. 15). It is not clear why megaripples were not formed here. Additional features in the study area include a sunken vessel at the toe of the shoreface at the northern boundary (Fig. 15, red arrow) and parallel beam trawling tracks (see the Supplementary material for details).

The results of the 2018 multibeam survey are comparable to the survey of the year before. However, the shore-normal trough-like features were less pronounced (0.05–0.4 m deep) and the sinuous erosional path between the spur and the shoreface was covered with sediment (Fig. 16, lower panel). In 2018, the Noordwijk area was surveyed at the end of a quiet spell which can explain the contrast of the results with the 2017 survey that was interrupted by storms. In 2018, the shore-normal gullies were much less distinct, which might be caused by inactivity of the gullies followed by sedimentation that fills in and levels out their morphology.

The mentioned shoreface spur is probably an outcrop of a clay or loam layer. The Noordwijk study area is situated at the location of the former mouth of the Old Rhine estuary, the main distributary of the river Rhine that was active between c. 5000 and 800 years ago. These estuarine deposits include clayey and loamy layers that resist erosion and can cause deviant morphodynamic behaviour. Box coring in 2018 of the sinuous erosion path (box core NW14; see Fig. 18) and the small-scale shoreface depressions showed the occurrence of compacted Holocene clays below a thin layer of sand. In case these clayey layers at the shoreface extend landward below the coastal dunes, they can act as aquitards and cause groundwater to seep from the shoreface, leading to destabilization and erosion of its deposits. The tongue-like depressions (Fig. 17 [3]) were possibly formed by such processes. However, downwelling currents, e.g. caused by wave set-up during high-energy events, are another potential cause for the formation of shore-normal trough-like features at the shoreface (e.g. [6] in Fig. 17). Erosion-resistant ridges (Fig. 17 [1]) will deflect the downwelling currents causing shore-oblique gullies such as [2]. In any case, these features indicate that between c. −12 m and −14 m seaward flow over the shoreface, and with that seaward transport of sand, is likely. Further investigation is needed to distinguish between the suggested mechanisms and gain information on the timing and extent of them.

### 4.3. Shoreface sediments

#### 4.3.1. Sedimentary structures

Transport processes create typical structures during sediment deposition. For instance, the orbital motion of waves and the migration of ripples under a uni-directional current produce specific but very

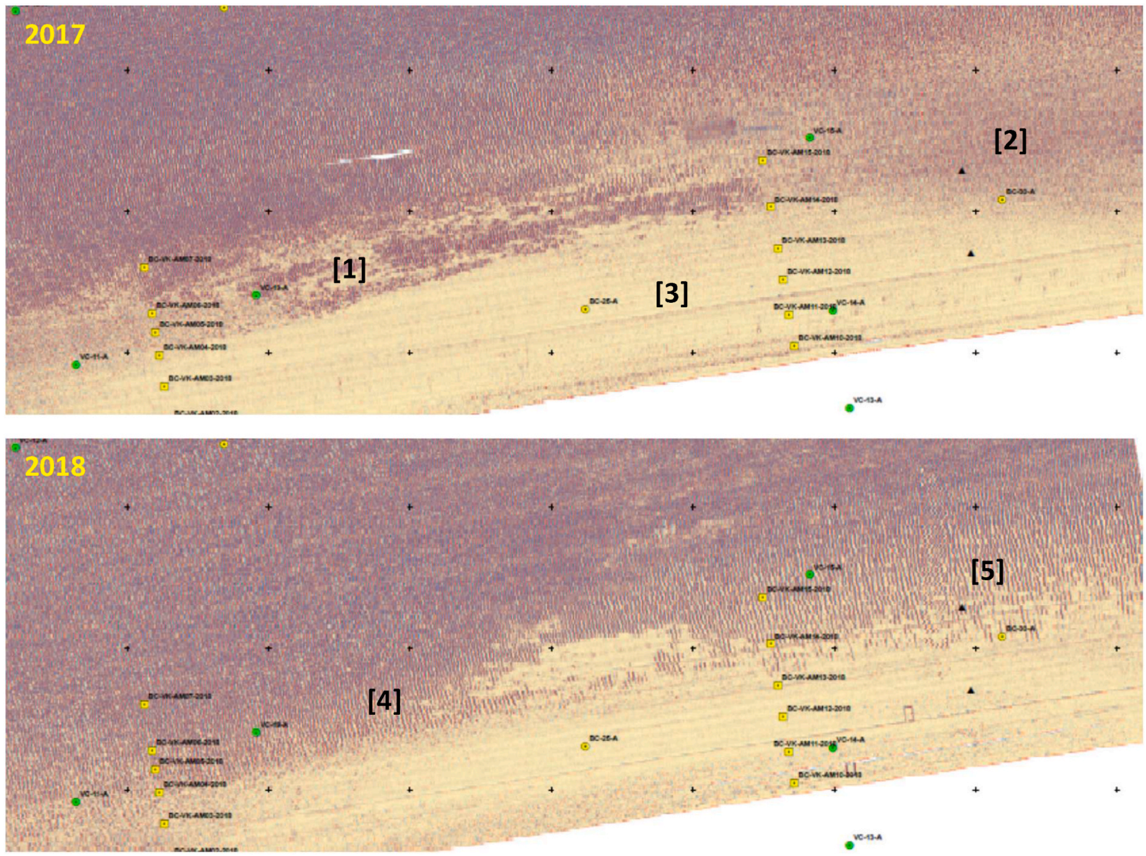


**Fig. 11.** Detrended multibeam bathymetry of the southern half of the Ameland Inlet study area in 2017 and 2018, showing different ripple patterns independently of depth. In 2017 (upper panel), the ripples became irregular when going in landward direction (to the bottom of the map; [1]). Toward the east (which is right in the figure) they became smaller [2]. Above −15 m they disappeared completely (white part of map; [3]). In 2018 (lower panel) the ripples became higher when going in landward direction (to the bottom of the map; [4]). In the east their spacing increased [5]. Changes occurred over a wider zone than in 2017. The positions of vibrocores (green dots) and box cores (yellow squares) are indicated.

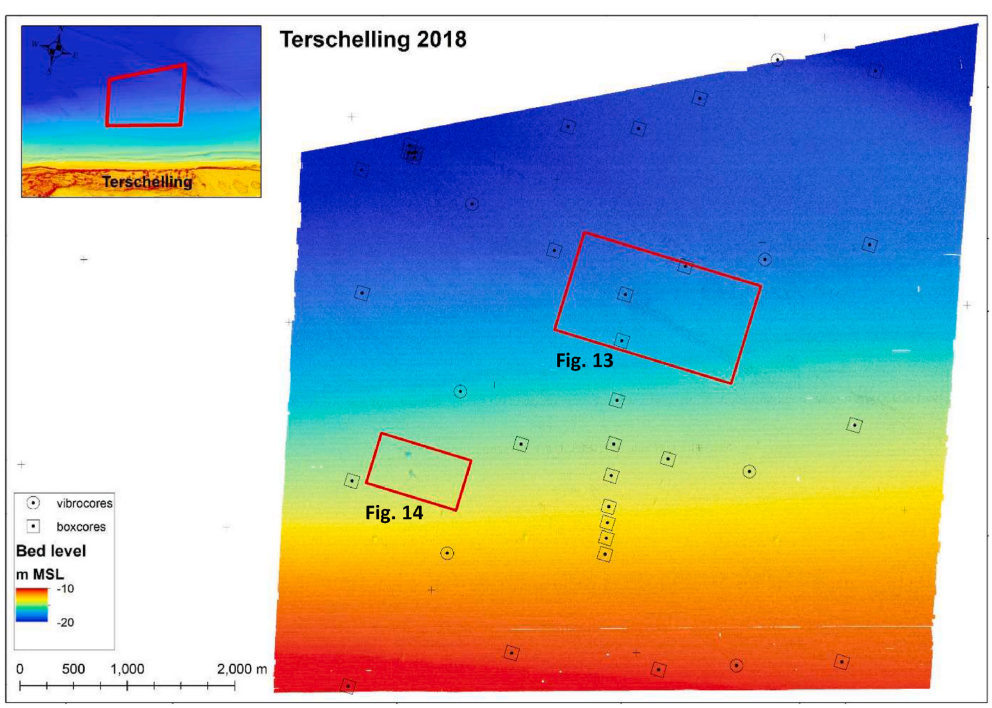


**Fig. 12.** Multibeam bathymetry of the Terschelling study area in 2018, depth ranging between −10 m and −20 m. The positions of vibrocores (circles) and box cores (squares) are indicated. Insets are the positions of Figs. 13 and 14.

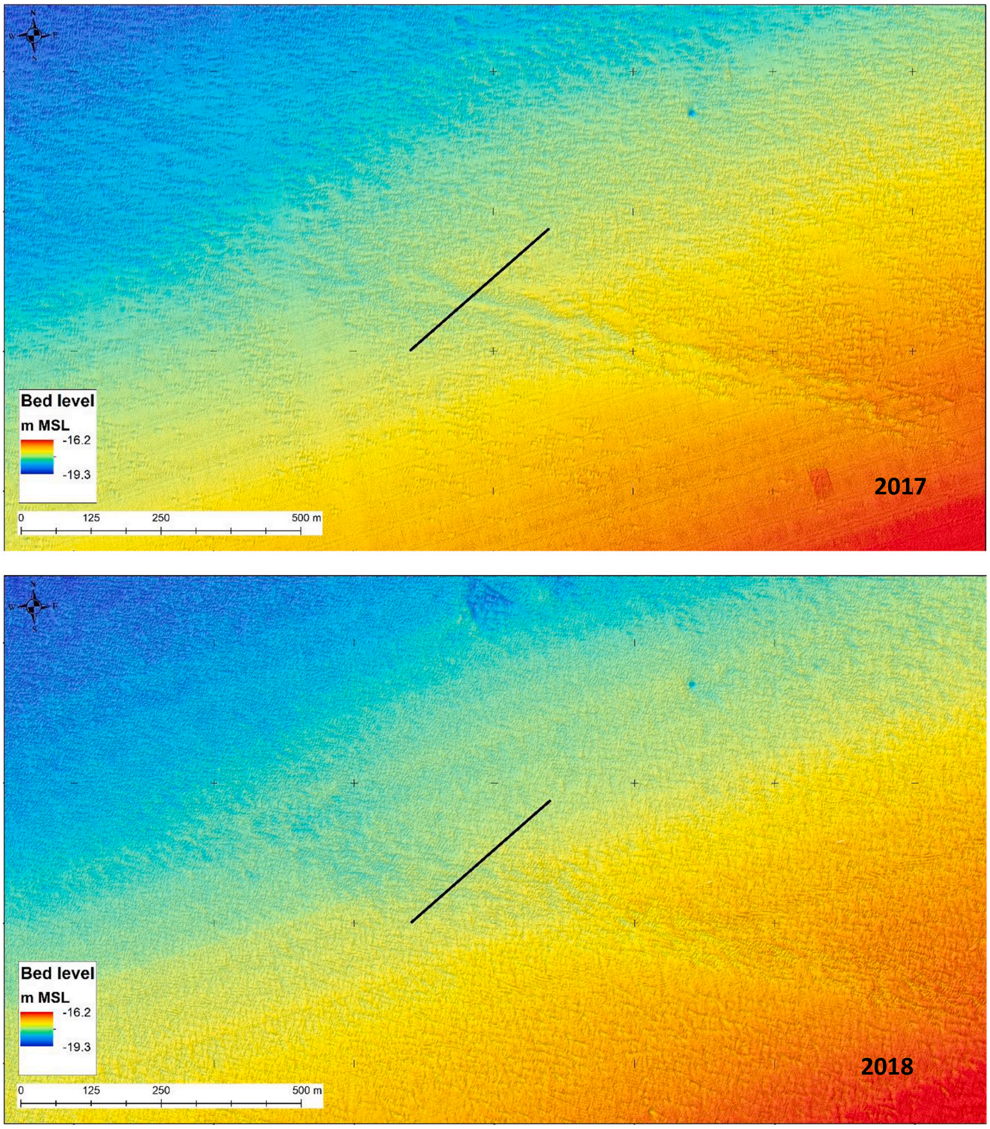


**Fig. 13.** Gully observed at the Terschelling shoreface between −15 m and −18 m in 2017 (top) and 2018 (bottom), see Fig. 12 for position. In 2018 the gully was less distinct than in 2017, probably due to infilling with sand during calm conditions. The black lines indicate the position of profiles over the gully that are shown in the Supplementary material. The gully possibly guides seaward flowing water and sediment over the shoreface. The upper parts of the maps show depressions (pockmarks?) that are more distinct in 2018. See text for explanation.

different structures. Burrowing animals tend to mix sediments and destroy sedimentary structures. The most abundant burrower is the Common Heart Urchin (*Echinocardium cordatum*), a sea urchin that migrates laterally through the sediment and thus erases the structures formed by physical processes (see Fig. 19; and Reineck and Singh, 1980, Fig. 240). The variation in sedimentary structures illustrates the variability in seabed processes in the study areas. The sediments in the box cores are part of the active layer (see Section 4.1).

The box cores from the Ameland Inlet study area show an upper layer of bioturbated sediment and a cross- and parallel bedded lower part that are separated by an undulating erosional surface. The upper layer is 0.04–0.11 m thick and usually has a shell lag at its base. Down to c. 16 m depth, the upper layer is completely burrowed, with abundant living specimen of sea urchins and *Ensis directus*, the American Jack-knife clam (core AM13, Fig. 18; core AM10, Fig. 20, left panel). Between 16 and 18 m depth, bioturbation is incomplete. The bioturbated upper layer shows mud percentages up to 6%. It indicates a calm period without transport of sand by currents. The lower part shows large- to small-scale cross-bedding and parallel bedding formed by migrating (mega-) ripples. Cross-bedding can be bi-directional which indicates reversal of the current direction, typical for tidal currents. Core AM14 (Fig. 20, right panel) shows an alternation of sand and clay layers that is caused by variation in current velocities: sand is transported by (strong) currents, clay settles during calm periods. Such variations can for instance be caused by the spring tide-neap tide cycle.

Box cores from Terschelling also show a bioturbated upper part and a bedded lower part, separated by an undulating erosional surface. The upper layer is 0.04–0.10 m thick and shows traces of burrowing animals. Between 13 m and 17 m depth (cores TS04-TS06) all physical structures have been destroyed. The most abundant burrowers are *Echinocardium* and *Ensis*, the latter being less abundant than in the Ameland area. Both layers show parallel bedding and cross-bedding, sometimes bi-directional, which indicates reversing tidal currents. Locally, beds with upward curving layers ('swaley bedding') occur. Swaley bedding is formed by the combination of a unidirectional flow and wave oscillations during deposition and suggest the impact of storm waves on the seabed (Fig. 21, right panel).

Box cores from Noordwijk show foresets of larger ripples, sometimes in opposing directions (indicating current reversals), overlain by a partly bioturbated layer. The upper layer is up to 0.16 m thick and locally contains a shell lag at its base (Fig. 22). At the shoreface below 15 m depth and in the adjacent trough, the top layer is strongly burrowed by sea urchins. *Ensis* is much less abundant than in the study areas along the Wadden coast. This layer contains 2–7% mud with values peaking at 10–12% between 14 m and 16 m depth (Fig. 22, left panel).

Box cores from the shoreface near the erosion structures described in

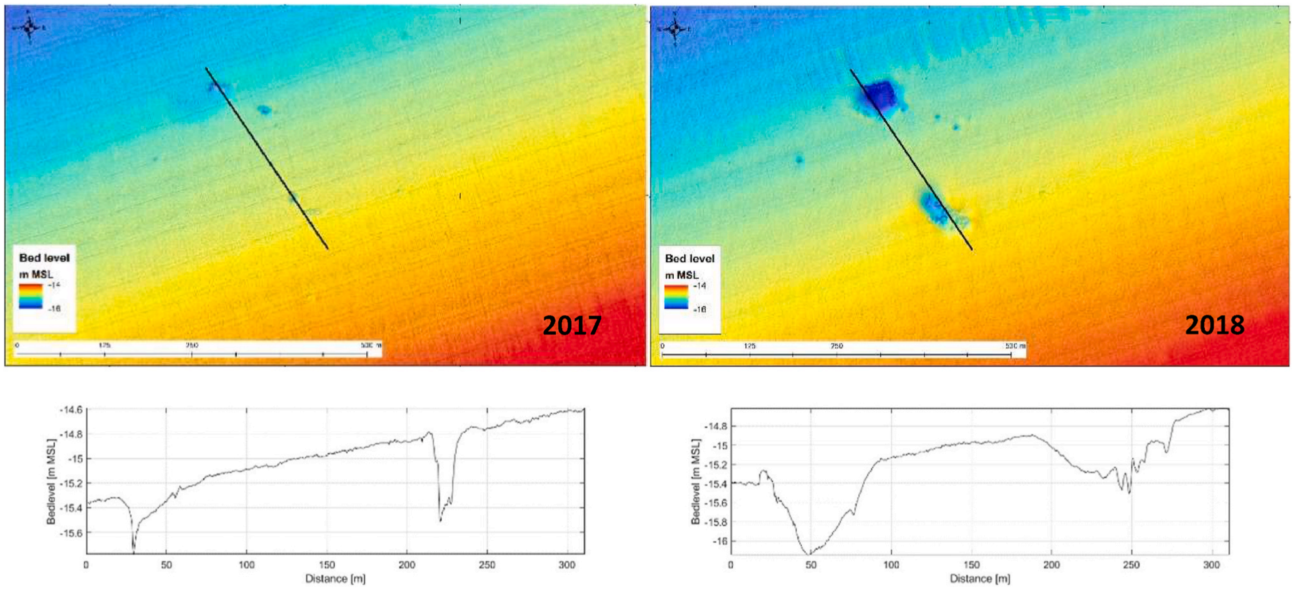


**Fig. 14.** Pockmarks at the lower shoreface of Terschelling at c. −15 m depth, see Fig. 12 for location. In 2017 the pockmarks were about 0.5 m deep and 20 m in cross-section, in 2018 they were about 1 m deep and 40 m in cross-section. Pockmarks are formed where gas or fluids escape from the seabed. The black lines indicate the position of the profiles crossing the pockmarks that are shown in the lower panels (see also the Supplementary material). See text and Oost et al. (2019b) for details and discussion.

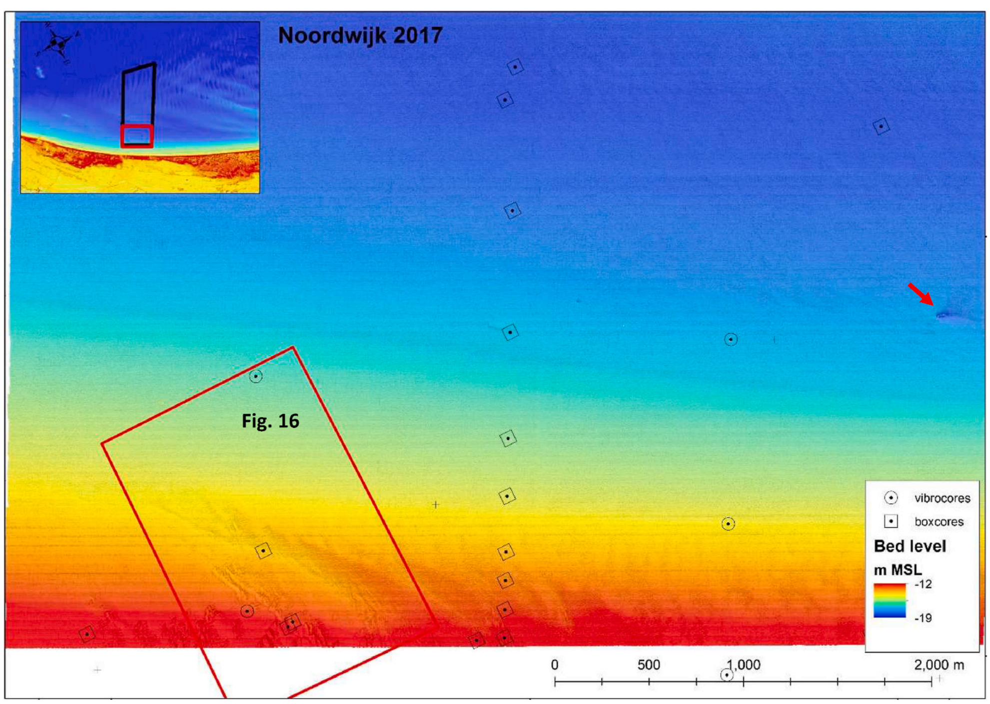


**Fig. 15.** Multibeam bathymetry of the inshore part of the Noordwijk study area in 2017, depth ranging between −12 m and −18 m. Inset shows the position of Fig. 16. The red arrow indicates the position of a sunken vessel. The positions of vibrocores (circles) and box cores (squares) are indicated.

4.2.3 show a thick consolidated clay layer with a thin, slightly muddy sand layer on top (Fig. 18, middle panel; Fig. 22, right panel). The consolidated clay represents an older Holocene deposit that likely is related to the mouth of the Old Rhine estuary (see de Haas et al., 2018; for more information).

*4.3.2. Grain-size distributions*

The grain-size distributions of the surface sediment samples can be grouped according to the main morphological units in the study areas. In all areas the grain sizes in the nearshore area (shoreface, delta front) are finer than in the offshore area. This division is present in the samples from both surveys. Table 6 shows the average values and ranges of the $D_{50}$ and sorting of the grain-size distributions. Note that grain-size classification follows the Wentworth scale (fine-grained sand: 125–250 μm; medium-grained sand: 250–500 μm). For details on the grain-size analyses, see Oost et al. (2019a).

The delta front in the Ameland Inlet study area consists of well-sorted (with exception of 2 (very) poorly sorted 2017 samples), fine-grained

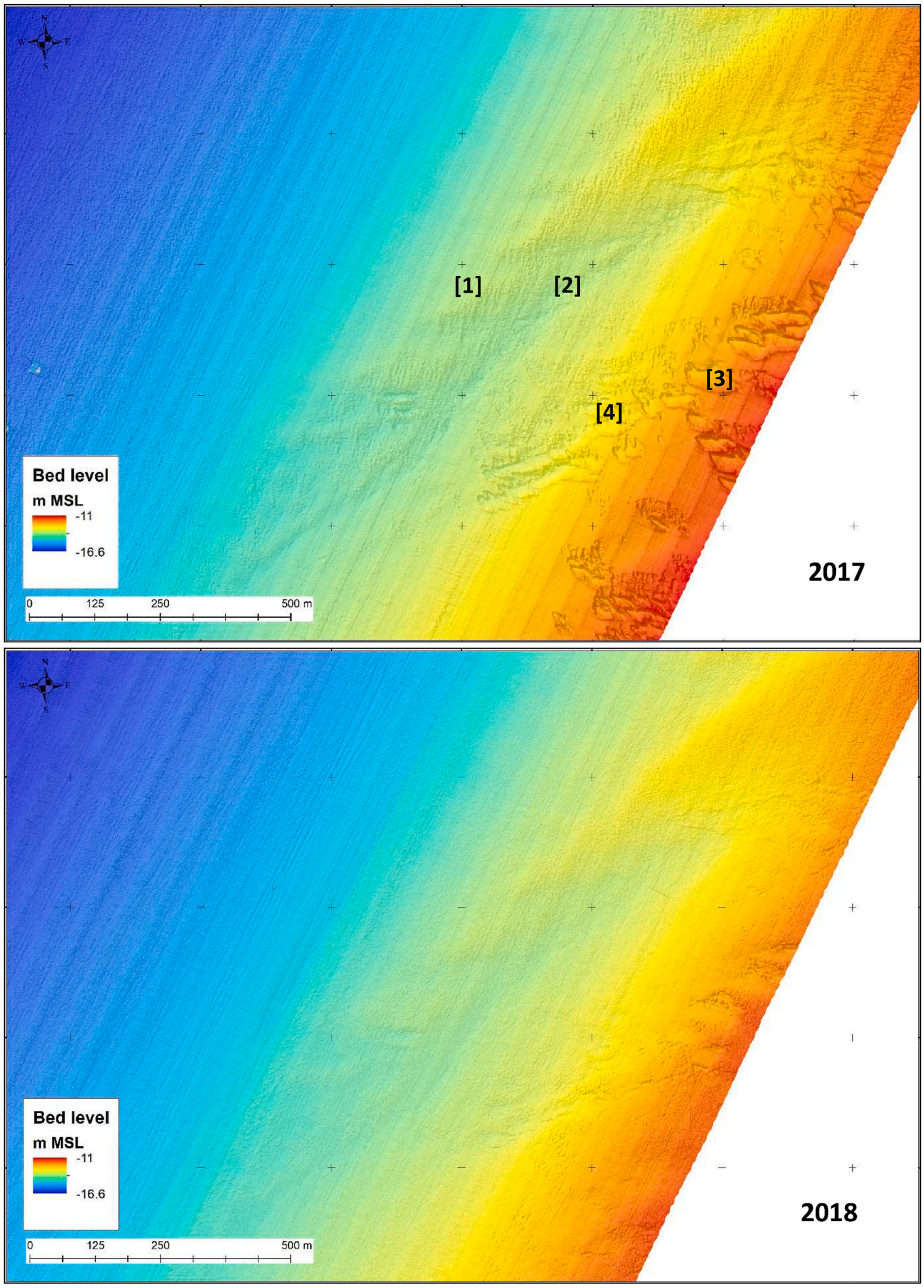


**Fig. 16.** The spur-like extension [1], the associated gully [2] and 'scars' [3], [4] observed in the Noordwijk shoreface. The morphology is clear in 2017 (top panel) but less distinct in 2018 (bottom panel). Infilling with sand during inactivity is the likely cause of the smoothing of the features. See text for explanation.

sand ($D_{50}$: 165–248 μm) with varying mud content. In 2017 only 2 samples between 14 and 15 m depth contained mud (9 and 17%), in 2018 all samples but one between 11.5 m and 18 m depth contained 4–7% mud. The sand from the deepest part of the delta front and the offshore seabed is slightly coarser ($D_{50}$: 216–232 μm) than the delta front. It is (very) well sorted and does not contain mud.

The shoreface of the Terschelling study area comprises well-sorted, fine-grained sand (range: 197–237 μm) down to 18 m depth. The offshore area is slightly coarser (range: 229–304 μm, average 247 μm) and for the most part well sorted. This area lacks mud in the seabed sediments. The sand at the seabed offshore Terschelling is slightly coarser than that offshore Ameland Inlet.

Grain sizes along the Holland coast are in general coarser than along the Wadden coast. Sediments from the shoreface and the adjacent trough at Noordwijk are comparable; down to a depth of 18 m moderately to poorly sorted medium-grained sand with up to 7% of mud occurs. The median grain sizes fall in the range 217–323 μm, with an average value of 273 μm. In 2018, samples between 14 and 17 m depth contained 10–12% mud. The mud content of the surface sediments is likely related to the high inshore mud concentrations near the seabed along the Holland coast (see van der Hout et al., 2015; for more information).

Going further offshore, the ridges and sand waves consist of coarser but well-sorted sand (331–414 μm, average 357 μm). Mud (2%) is found

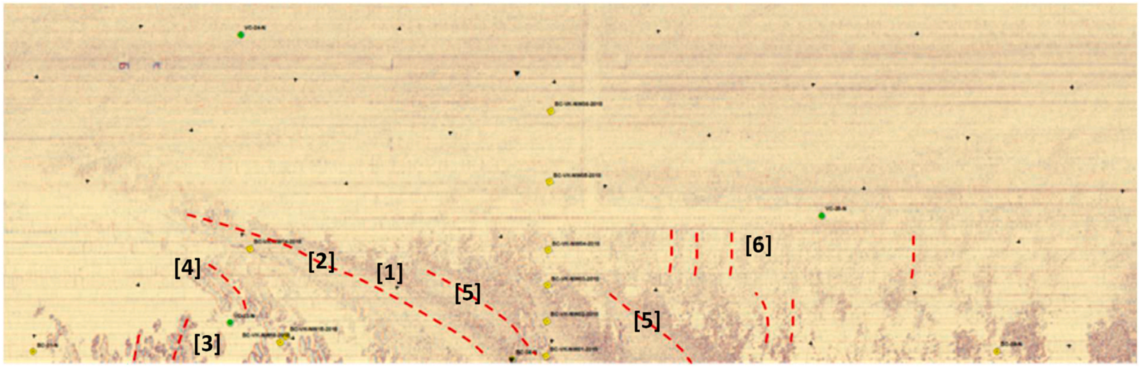


**Fig. 17.** Detrended image of the lower half of Fig. 15, showing small-scale morphology at the Noordwijk shoreface in 2017. A darker colour indicates a positive topography, gullies are indicated by dashed lines (note that not all features have been indicated). Indicated are the 'spur' [1], its associated erosional gully [2], tongue-like depressions [3], other shore-oblique gullies [4], [5] and small shore-normal gullies [6]. Top of figure is seaward, bottom is landward. The positions of vibrocores (green circles) and box cores (yellow squares) are indicated. See text for discussion.


**Fig. 18.** Rectangular box cores collected in 2018 with the side detached. Box core TS16 (NW corner Terschelling area; left panel) shows a coarse-grained shell layer. Box core NW14 (Noordwijk area; middle panel) shows a sand layer overlying a stiff blue-grey clay. Box core AM13 (delta front, Ameland Inlet area; right panel) shows a layer of brown, oxygenated sand on top of dark grey sand that is poor in oxygen. Directly left of the yellow label sits a razor clam that has dug itself in, probably in reaction to the penetration of the corer into the seabed and its subsequent extraction. Scale in cm.

**Fig. 19.** Box core AM08 from the seabed seaward of the delta front in the Ameland Inlet study area. The brown-beige top layer overlies a dark grey layer of anoxic sand. The grey-black circles are traces of the sea urchin Echinocardium cordatum that moves sideways through the sediment. Scale in cm.

in only one sample. In the sand wave field, an occasional sample with a significantly coarser grain-size distribution occurs. In general, the sand on the ridge is slightly better sorted than that in the sand wave field.

The variation in grain sizes between both nearshore and offshore areas and between the study areas is likely related to the variation in underlying deposits. For instance, the coarser sand and poorer sorting in the Noordwijk area can be caused by the comparatively coarse alluvial deposits of the river Rhine that are being eroded in the shoreface and trough. The sands farther offshore reflect this source as well but the continuous transport by tidal currents will have improved the sorting of these sediments. There are no indications that the offshore seabed erodes so the input of 'freshly' eroded alluvial sand is supposedly very small.

### 4.4. *Decadal-scale evolution of the lower shoreface*

The Jarkus database of yearly shoreface profiles measured since 1965 enables the analysis of shoreface evolution over 50 years. Plotting the yearly profiles shows the year-to-year variation. The variation decreases with increasing water depth. Jarkus profile 82.00 (Fig. 23) at the northern boundary of the Noordwijk study area is representative for the development of the Holland coast and shows several developments. The profile above NAP -7 m shows the changes caused by migrating breaker bars and shoreface nourishments. Moreover, a large beach & shoreface nourishment placed in 2007–2008 shifted the beach significantly seawards. The profile below NAP -7 m shows a gradual landward retreat. Between 1965 and 2015, the −10m contour shifted c. 225 m landward. At the 1965 location of the −10m contour, the seabed has deepened almost 1 m. This development is representative for the larger part of the Holland coast (compare Table 7). What causes this deepening of the lower shoreface, is not understood, nor where the sediment volume was transported. It can be transported either along shore or cross-shore. This eroding part of the lower shoreface produced about 100 million $m^3$ between 1965 and 2015 (length c. 100 km, width c. 1 km, vertical offset 1 m; see Fig. 23), which is about 2 million $m^3$ per year. In case this sediment volume was moved upwards into the upper shoreface, this was by far not enough to maintain the shoreline. Since the introduction of

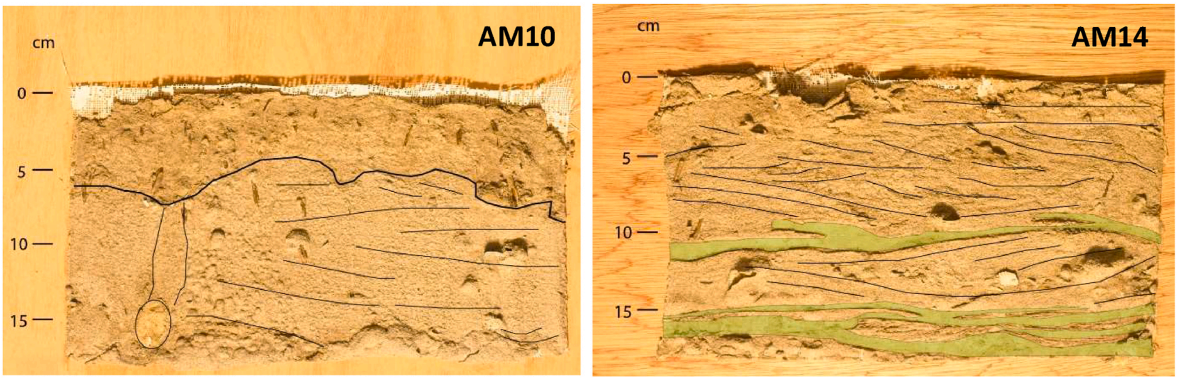


**Fig. 20.** Lacquer peels of box cores AM10 (11.7 m depth), left, and AM 14 (17.8 m depth), right, from the Ameland Inlet study area. Peel AM10 shows a muddy top layer that is completely homogenised by burrowing and that erosively overlies cross-bedded sand. In the top layer abundant juvenile American jack-knife clams occur. The left side of the panel shows a downward escape burrow of a Common Heart Urchin, with the dead animal (oval) at the end. Peel AM14 shows structures such as bi-directional foresets which indicate two current directions. The alternation of sand and clay layers (yellow) is caused by changing current velocities: sand is transported by (strong) currents, clay settles during calm periods.

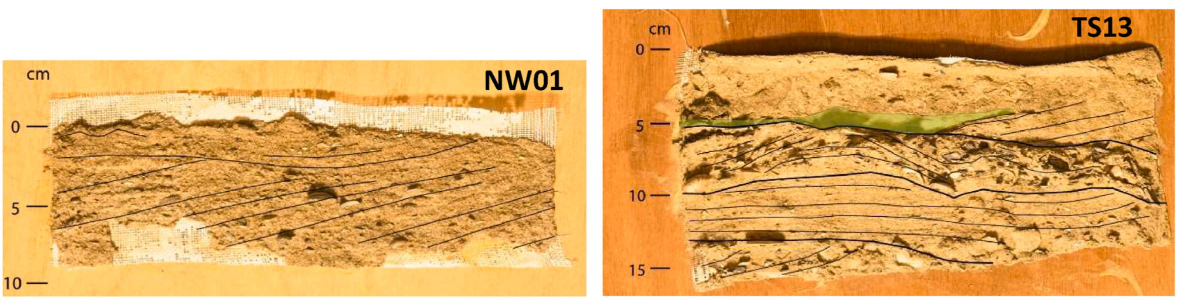


**Fig. 21.** Lacquer peels of box cores NW01 (11.9 m depth) from the shoreface of the Noordwijk study area, left, and TS13 (20.3 m depth), right, from the Terschelling study area, both showing examples of 'swaley' bedding. Peel NW01 shows regularly cross-bedded sand with some shells, overlain by a sand layer characterized by upward curving laminations. Peel TS13 shows foresets at the base that are truncated by parallel to swaley bedding truncated by a distorted shell layer. The distorted shell bed indicates wash-out and even higher-energy conditions, the shells are a lag deposit. The overlying sand and clay layers were formed after waning of the storm by alternating tidal currents.

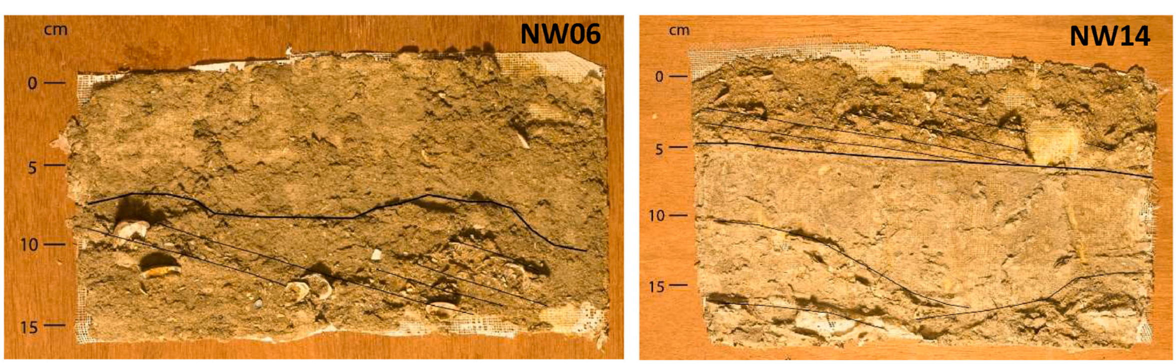


**Fig. 22.** Lacquer peels of box cores NW06 (15.8 m depth), left, and NW14 (13.8 m depth), right, from the Noordwijk study area. Lacquer peel NW06 shows shell-bearing foresets formed by a current that are truncated by a muddy, strongly bioturbated deposit. The top layer contains 12% mud. Peel NW14 shows a compact clay layer with poorly sorted sand layer on top. Compare the peel with the sediment core shown in Fig. 16, middle panel. Note that lacquer does not penetrate clay, so the clay is missing from the peel.

the policy of Dynamic Conservation in 1990, over 150 million $m^3$ of sand (beach and shoreface nourishments 1990–2015, excluding the Sand Motor experiment but including reinforcements of coastal towns and sea dykes; data Rijkswaterstaat) has been added to the Holland coast, which is on average more than 6 million $m^3$ per year, to stop coastal recession.

### *4.5. Shoreface processes and sand transport*

Both field observations and numerical modelling are used to highlight processes, such as tidal and residual flows and waves, and sand transport in the lower shoreface. Observations usually give an accurate picture of processes but are limited in time and space. Models, on the other hand, generate a more complete temporal and spatial coverage but they are schematizations of reality. However, models facilitate scenario studies, e.g., to assess the effects of a single storm.

**Table 6**
Range and mean value (in bold) of median grain-sizes and sorting of the surface sediment samples as measured with a Malvern Mastersizer. Sorting is defined as $D_{60}/D_{10}$, values smaller than 1.80 are classified as 'well sorted', values in the range 1.80–2.19 classify as 'moderately sorted', larger values indicate poor sorting. The range and mean value (in bold) of mud percentages of the samples are given; note that not all samples contain mud. For details on the grain-size analyses, see Oost et al. (2019a).

| Study area | 2017 | | | | | 2018 | | | | |
|---|---|---|---|---|---|---|---|---|---|---|
| | $D_{50}$ sand (μm) | sorting | n | mud (%) | n | $D_{50}$ sand (μm) | sorting | n | mud (%) | n |
| **Ameland Inlet** | | | | | | | | | | |
| Deltafront | 165-**199**-222 | 1.61–**2.78**-7.79 | 6 | 9-**13**-17 | 2 | 174-**209**-248 | 1.64–**1.74**-1.85 | 13 | 4-**5**-7 | 9 |
| offshore seabed | 216-**224**-232 | 1.47–**1.49**-1.54 | 8 | 0 | 0 | 222-**225**-231 | 1.47–**1.49**-1.53 | 3 | 0 | 0 |
| **Terschelling** | | | | | | | | | | |
| Shoreface | 197-**210**-237 | 1.61–**1.66**-1.70 | 8 | 0 | 0 | 208-**217**-229 | 1.61–**1.68**-1.70 | 8 | 0 | 0 |
| offshore seabed | 229-**250**-304 | 1.53–**1.58**-1.70 | 8 | 0 | 0 | 230-**244**-256 | 1.60–**1.75**-2.02 | 8 | 0 | 0 |
| **Noordwijk** | | | | | | | | | | |
| shoreface & trough | 222-**282**-323 | 1.80–**2.04**-2.46 | 6 | 3-**5**-7 | 5 | 217-**269**-313 | 1.94–**2.97**-6.73 | 12 | 2-**6**-12 | 12 |
| ridges & offshore | 331-**362**-414 | 1.55–**1.69**-1.86 | 6 | 2 | 1 | 335-**349**-366 | 1.60–**1.65**-1.76 | 4 | 0 | 0 |

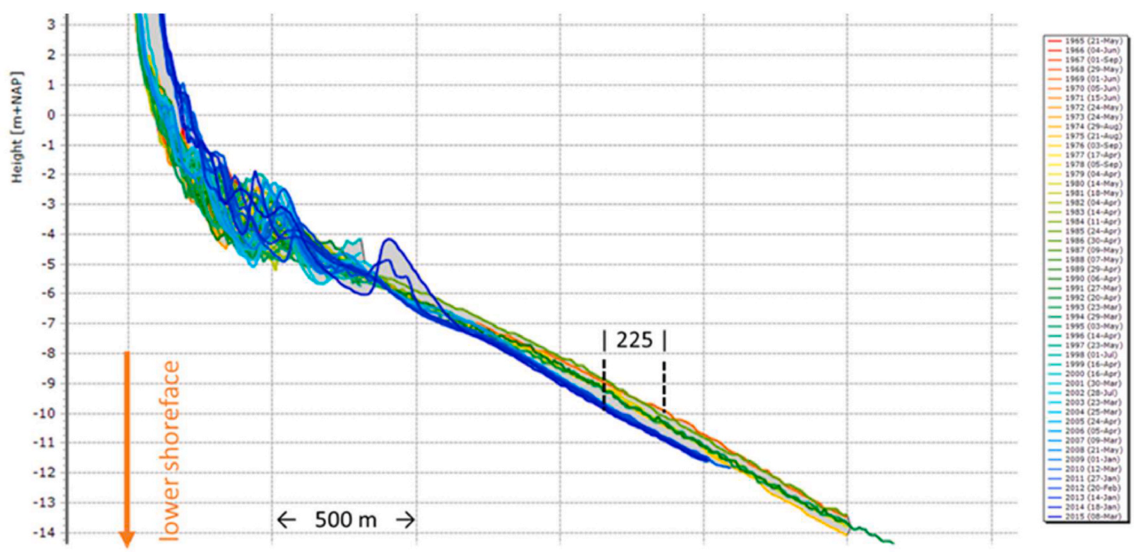


**Fig. 23.** Evolution 1965–2015 of Jarkus profile 82.00 at Noordwijk. The upper part of the profile (depth < −7 m) shows migrating breaker bars and shoreface nourishments. A large beach & shoreface nourishment at Noordwijk in 2007–2008 shifted the upper profile seaward. Below NAP -7 m, the profile retreated gradually.

**Table 7**
Regional development trends of the Dutch lower shoreface. The information is based on descriptions in the following publications: Elias et al. (2012; 2017); van Alphen and Damoiseaux (1987); van der Spek and Lodder (2015). Legend: − = erosive; (−) = slightly erosive; 0 = stable; (+) = slightly accreting; + = accreting; ? = unknown/no data.

| Coastal section | Lower shoreface | | Width zone |
|---|---|---|---|
| | -8m → −12m | −12m → −20m | −10m → −20m |
| Western Scheldt mouth | (−) | (−) | wide |
| Eastern Scheldt mouth | (−) | (−) | variable |
| Ebb deltas Grevelingen, Haringvliet | (−) | 0 | wide |
| Maasvlakte | (−) | (−) | ? |
| Hook of Holland - Katwijk | (+) | (−) | wide |
| Katwijk - Egmond | (+) | (−) | narrow |
| Egmond – Grootte Keeten | ? | (−) | wide |
| Ebb delta Texel Inlet | – | ? | variable |
| Ebb delta Vlie inlet | – | ? | variable |
| Wadden – other ebb deltas | 0 | 0 | narrow |
| Wadden – barrier island coasts | 0 | 0? | very wide |

### *4.5.1. Observations*

*4.5.1.1. Residual flow.* The observed variation in residual flows is based on depth-averaged and low-pass filtered ADCP measurements at 20, 16/14 and 12/10 m water depth in the study areas. In general, it can be stated that residual flows are small under calm conditions, increasing in strength with decreasing water depth, and that longshore residual flows are larger than cross-shore residual flows. The direction of the residual flow depends on location and wave conditions and varies between places. At Ameland Inlet residual flows are typically eastward under calm conditions. During storm conditions (e.g., 20 November 2017; 4 m waves from NW; Fig. 24), we observed an increased eastward and landward residual flow. During an easterly storm with waves from north-east on 18 March 2018 at Terschelling (Fig. 25), the residual flow was landward and westward.

*4.5.1.2. Wave climate at 20m depth contour.* The wave climate information is based on wave buoy measurements at the offshore stations IJmuiden, Europlatform, Eierlandse Gat and Schiermonnikoog North (water depths respectively 21 m, 32 m, 26 m, 19 m) over the years 2013–2017. These observations have been translated to the 20m depth contour for the entire Dutch coast using a wave transformation matrix. Wave data measured at Noordwijk and Ameland Inlet during the field campaign were used to validate the transformation results.

The mean significant wave height $Hm0$ increases from about 1.1 m

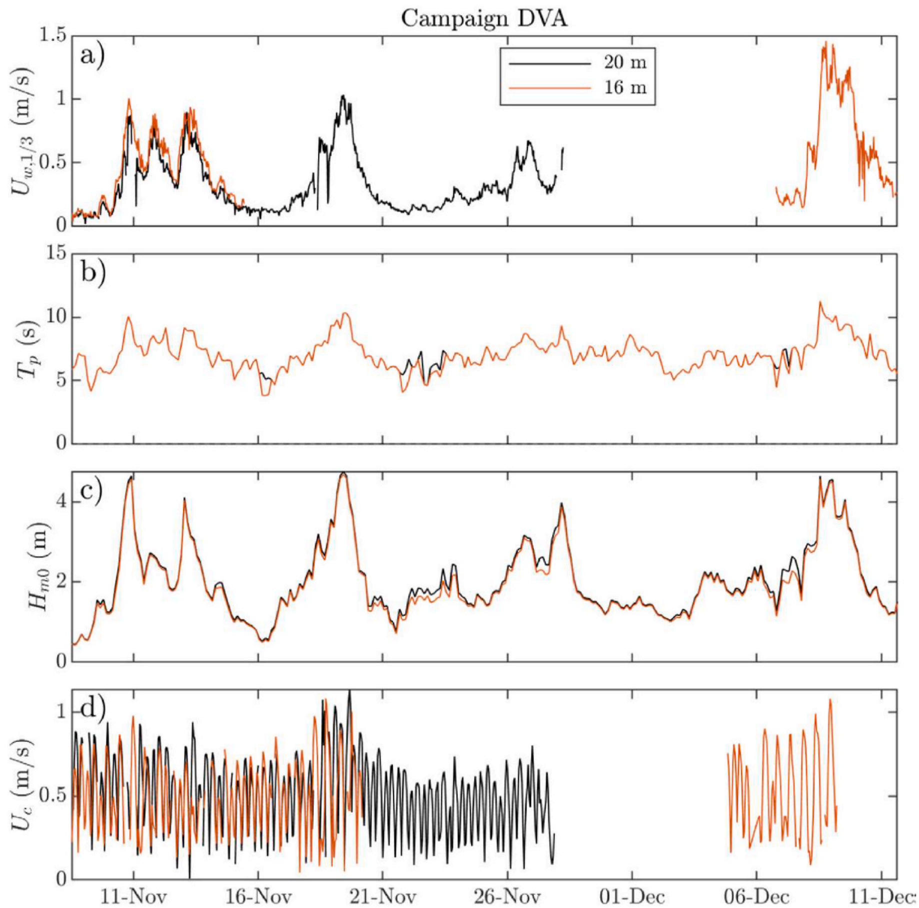


**Fig. 24.** Observations of flow and waves at the Ameland Inlet study area between 10 November and 11 December 2017 at water depths of 16 m (orange) and 20 m (black). During this period four high-wave events occurred. The figure shows time-series of, from top to bottom, (a) orbital velocity amplitude, (b) peak wave period, (c) significant wave height and (d) depth-averaged current velocity magnitude.

near Zeeland to about 1.3 m near Texel. In Zeeland, the significant wave height H*m*0 was larger than 2.0 m during 10% of the observation interval. Near Texel, this value is about 2.3 m. The maximum wave height increases from about 5.5 m near Zeeland to about 7 m near Schiermonnikoog.

*4.5.1.3. Orbital velocities and small-scale bedforms.* Schrijvershof et al. (2019) and Van der Werf et al. (2022, this issue) present new data of near-bed orbital velocities and small-scale bedforms measured simultaneously at various depths and locations on the DLSF.

Orbital velocities under waves were measured at the lower shoreface in the study areas using an ADV at 20 m and 16/14/12 m water depth. Near-bed orbital velocities increase with wave height and decrease with water depth. They can be reasonably well described by linear wave theory. The velocity skewness $S_k$ is generally positive, which means that higher velocities occur in the direction of wave advance. This indicates a potential for wave-driven sand transport in landward direction.

During the measurement campaign at Ameland Inlet (Fig. 24), the near-bed orbital velocities reached a value of about 1 m/s at the deepest frame and 1.5 m/s at the shallow frame under energetic wave conditions (wave height H*m*0 > 3 m; van der Werf et al., 2022, this issue). At Terschelling (Fig. 25), the orbital velocity amplitude $U_W$ exceeded 1 m/s during high wave events (e.g., 18 March; significant wave height $H_s$ at −14m c. 2.5 m). The calculated wave-related Shields parameter indicates a plane bed/sheet-flow regime at the seabed for these conditions (see van der Werf et al., 2022, this issue).

Ripple heights ranged between 0.01 and 0.03 m and ripple lengths between 0.08 and 0.20 m. Note that the sonar could not measure the bed in sheet flow conditions as the abundant sediment suspension blocked the acoustic signal. Ripple dimensions are controlled by wave mobility, with lower and shorter ripples for higher waves, and not so much by the tidal currents. The measurements clearly indicate significant sediment mobility at the lower shoreface under higher wave events. It is yet unclear what this means for the net sand transport.

*4.5.2. Modelling*

The development of the KG2 lower shoreface model of the Dutch coast (outlined in section 3.3) and the results as calculated over the years 2013–2017 are described in detail by Grasmeijer et al. (2022, this issue). Here, we present a concise summary of the results.

*4.5.2.1. Current velocities at the 20m depth contour.* From south to north, the mean depth-averaged peak flood velocity increases along the Delta coast, it is low off Scheveningen and increases again along the Holland coast. The largest value (0.84 m/s) is observed near Texel and decreases towards Schiermonnikoog (see Fig. 26 for locations). The largest mean peak ebb velocity (0.73 m/s) is observed near Westkapelle and decreases towards the north-east. This causes the flood-dominant tidal velocity asymmetry to increase from south to north up to Texel and to decrease towards Schiermonnikoog.

Residual velocities are calculated with real-time tidal and meteorological forcing and freshwater discharges (including salinity). The surface residual flows are alongshore directed with maximum values of 0.14 m/s at the northern part of the Holland coast. In the Delta area, they are directed offshore. The near-bed residual flows are 0.01–0.02 m/s strong and are onshore-directed. Near Texel and Terschelling, they are

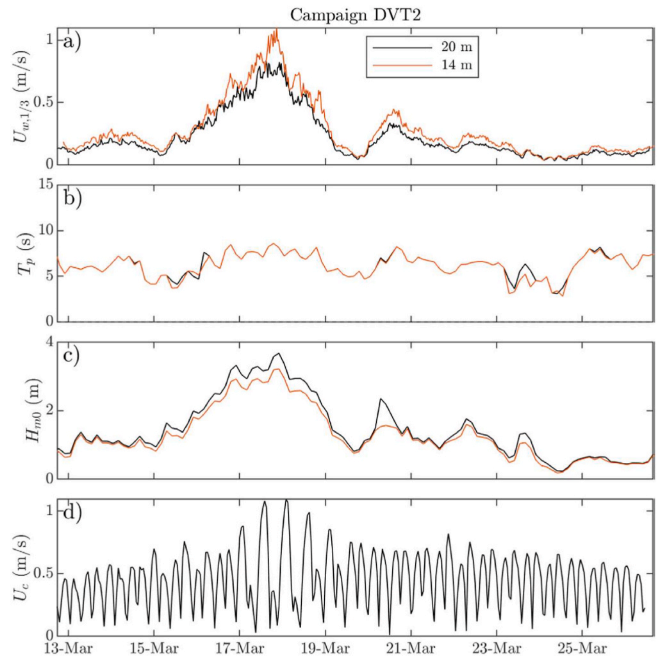


**Fig. 25.** Observations of wave orbital velocities at the Terschelling study area between 13 and 27 March 2018 at water depths of 14 m (orange) and 20 m (black). The figure shows time-series of, from top to bottom, (a) orbital velocity amplitude, (b) peak wave period, (c) significant wave height and (d) depth-averaged current velocity magnitude.

shore parallel. The depth-averaged residual flow increases from 0.01 m/s near Zeeland to 0.07 m/s near Texel and decreases again to 0.02 m/s near Schiermonnikoog. This flow is in most cases parallel to the shore.

*4.5.2.2. Total net annual cross-shore sand transport.* Grasmeijer et al. (2022, this issue) state that the net annual sand transport rates along the Dutch coast are determined by the peak tidal velocities and their asymmetry, the density-driven residual flows (that are onshore near the seabed), the wind-driven residual flows (that are predominantly offshore near the seabed) and waves. The effects of density difference and wind on the 3D flow structure cannot be neglected along the DLSF. The effect of density is larger than that of wind.

The calculated annual net sand transport at the 20m depth contour is directed to the north-east, due to tidal asymmetry and residual flow. The alongshore-directed sand transport is much larger than the cross-shore sand transport, averaging ~100 $m^3$/m/year and ~10 $m^3$/m/year, respectively. Near-bed density-driven currents typically cause onshore-directed sand transport. The largest transports at the 20m depth contour occur along the northern part of the Holland coast, between Callantsoog and Texel (Fig. 26). Here, transport is parallel to the coast or directed to deeper water. Transports along the other parts of the coast are directed to shallower water.

Table 8 shows the total volumes of annual onshore directed transports over several depth contours along the Dutch coast. The annual shoreward transport over the 20m depth contour is 3.6 ± 0.9 million $m^3$. The cross-shore transports increase with decreasing water depth due to increased sediment stirring by waves and increased wave-related sand transport. Including return flow would reduce the annual onshore directed transports with c. 0.6 million $m^3$. The effect of grain size on the calculated annual transports is small (Table 8). Note that these volumes do not include the potentially large effects of severe (NW) storms that did not occur in the modelled 2013–2017 period.

The effect of storms on the net transport rates at the lower shoreface was investigated by assessing the contribution of different wave classes to the net cross-shore transport. A small net cross-shore transport during normal conditions caused by a near balance between onshore and offshore components about equal in magnitude, can be upset by waves higher than 3.5 m which causes a change in the net transport direction. This suggests that storm conditions play an important role for the net transport rates at the lower shoreface (Grasmeijer et al., 2022, this issue).

The almost doubling of the modelled total yearly cross-shore sand transport in shoreward direction from c. 3.6 million $m^3$ over the 20m depth contour to c. 7.1 million $m^3$ over the 16m depth contour (Table 8) implies a yearly erosion of 3.5 million $m^3$ of the area in-between. So far, structural erosion could not be established for the lower shoreface between −20 m and −16 m. An annual transport of 3.5 million $m^3$ over the 16m depth contour implies feeding of the shoreface above this depth. The net erosion of the lower shoreface of the Holland coast above −14 m (see Fig. 23) suggests that here, this annual supply is too small to compensate for the removed volume of sand.

## 5. Concluding remarks

### *5.1. New results*

The collected vibrocores confirm that the geological architecture of the lower shoreface of the Dutch coast varies considerably. The cores from Noordwijk confirm the general picture of a thin layer of active sediments overlying older Holocene lower shoreface and tidal channel deposits or Pleistocene river sands, illustrating the overall transgressive nature of the lower shoreface. The seaward front of the ebb-tidal delta at Ameland Inlet consists of ebb-delta channel deposits that lack the shell content of more regular tidal channel deposits. The cores from the Terschelling study area show that the lower shoreface here is underlain by deposits similar to those at the ebb-delta front of Ameland Inlet. This suggests that the lower shoreface of this study area was formed in the ebb-tidal delta of a precursor of Ameland Inlet and not in the transgressive setting of a retreating barrier island. These deposits were possibly formed as part of the ebb delta of the Middelzee, a large medieval precursor of the Ameland tidal basin. The active sediment layer in the Terschelling study area is comparatively thin and lacks mud, which suggests removal instead of redeposition of shoreface sediment following resuspension by storm waves. The stratigraphy of the lower shoreface, especially compacted Holocene and Pleistocene clay layers, where not covered by thick sand layers, are likely to have a strong effect on the shoreface bathymetry and morphodynamics.

The multibeam surveys of the study areas showed large-scale morphological patterns that were in line with expectations. The large-scale morphology of the lower shoreface seems rather stable, although the decadal time series of the Holland coast shows erosion: the part below −7 m deepened with c. 1 m in 50 years. On the other hand, the multibeam surveys showed details that have not been reported before. For example, in the 2017 the shoreface showed smaller-scale morphological phenomena such as pockmarks, shore-oblique gullies and ridges, and approximately shore-normal depressions. In 2017 the study areas were surveyed following or during energetic wave conditions and these small-scale features were likely exposed or even formed by the wave impact. Also, they are one way or the other related to the subsurface of the shoreface. The shore-obliques gullies and ridges at Terschelling and Noordwijk are likely outcrops of stiff older Holocene layers, some of the shore-normal depressions at Noordwijk turned out to be underlain by Holocene clay layers. All were most obvious after a stormy period which suggests that they are active under high waves and most probably are exposed or excavated by seaward near-bed currents, e.g., undertow. As such, these gullies and depressions suggest seaward sand transport under stormy conditions, although groundwater seepage could not be excluded for some of the depressions at Noordwijk. The pockmarks at the Terschelling shoreface are likely related to the natural gas reservoirs that have been discovered to the north of and underneath the island.

The different hydro-meteo conditions during the successive surveys

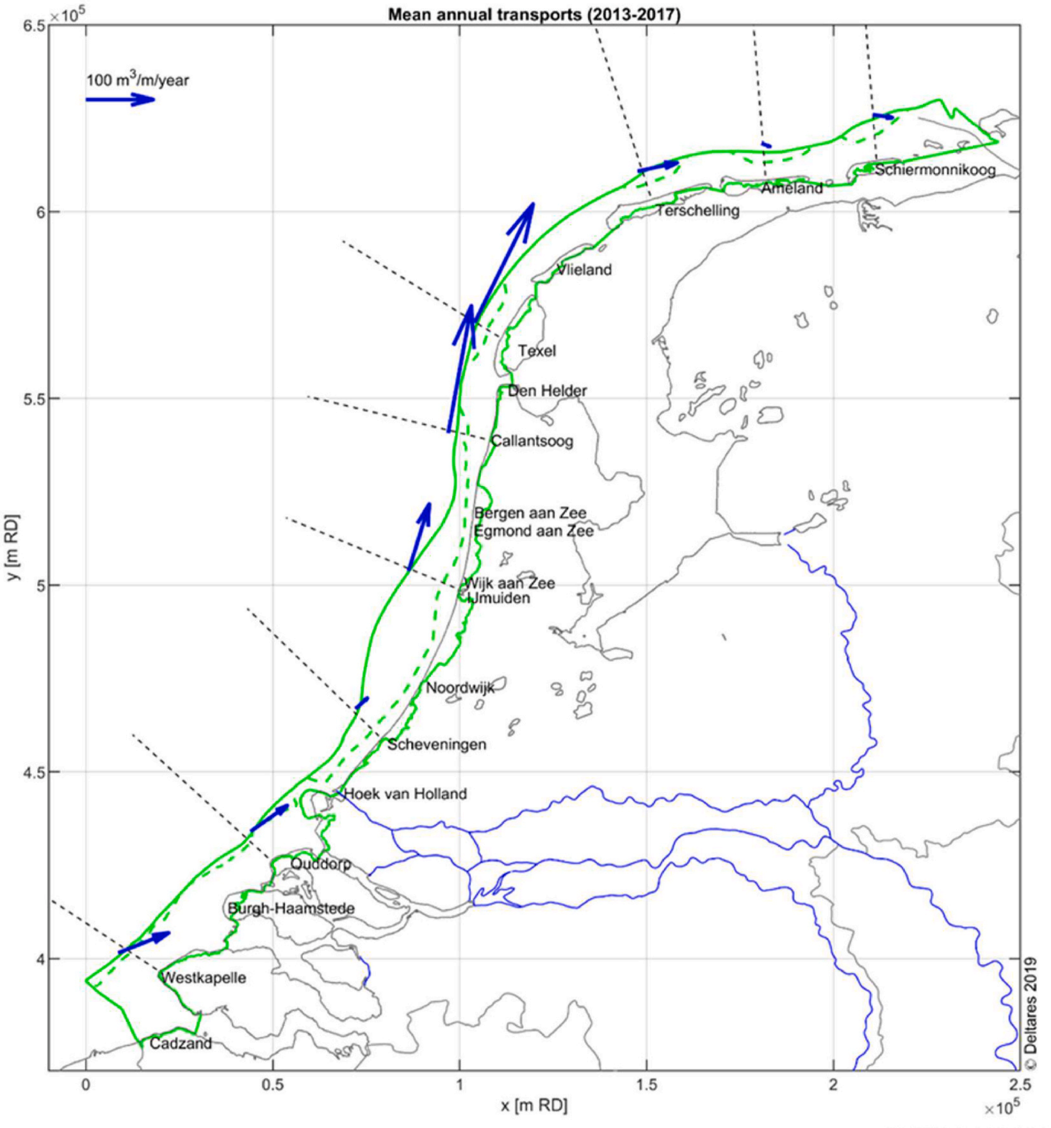


**Fig. 26.** Calculated mean annual sand transport at the 20m depth contour along the Dutch coast over the interval 2013–2017. The longshore transport is about 10 times larger than the cross-shore transport. The largest transport rates are calculated near Texel inlet. The solid green line depicts the boundary of the coastal foundation, the dotted green line shows the 15m depth contour.

**Table 8**

Calculated total net annual cross-shore sand transport in landward direction over the 20m, 18m and 16m depth contours along the Dutch coast (in million m$^3$). See text for model details. Results from Grasmeijer et al. (2022, this issue).

| Model setting | Grain size ($D_{50}$) | 20 m depth | 18 m depth | 16 m depth |
|---|---|---|---|---|
| no return flow | 250 | 3.6 ± 0.9 | 5.0 ± 1.4 | 7.1 ± 2.0 |
| return flow | 250 | 3.0 ± 0.8 | 4.3 ± 1.2 | 6.4 ± 1.9 |
| no return flow | 275 | 3.5 ± 1.0 | 4.9 ± 1.4 | 7.1 ± 2.1 |

can be recognized in the details of the seabed morphology. In general, the 2018 surveys were executed during calm weather. This resulted in a shift to shallower depth of the transition from two-dimensional megaripples to wave-influenced three-dimensional ripples at Ameland Inlet (which could be expected since shorter waves reach less deep so the maximum depth of wave impact on the seabed decreased) and infilling of the gullies and depressions at Terschelling and Noordwijk with sediment (as they were less or not active under those conditions). In contrast, the number of pockmarks had increased, and they were deeper and wider since they had not been infilled by sand on the move. Interestingly, the ripple patterns at the Terschelling and Ameland Inlet study areas differed from each other under both conditions, despite the short distance (c. 15 km), predominantly linear megaripples up to 0.5 m high at Ameland Inlet vs. compound, three-dimensional ripples up to 0.25 m high at Terschelling. This cannot be explained from the grainsize of the seabed sediment that at Ameland Inlet is only slightly finer and better sorted than at Terschelling, see Table 6. Variation in hydrodynamic conditions, shore-parallel tidal flow at Ameland Inlet vs. combined action of currents and waves at Terschelling, can explain these differences in seabed patterns.

In all study areas there is a division in grain-size distributions of the surface sediment samples between the nearshore area (shoreface, delta front) and the offshore area. The sand at the delta front at Ameland Inlet is in general finer but more variable in median grain size than that at the offshore seabed, although the value ranges of both areas overlap. The median grain size at the shoreface of Terschelling is smaller and hardly overlaps that of the offshore seabed. Moreover, the sand at the seabed at Terschelling is coarser and more poorly sorted than that near Ameland Inlet. Grain sizes along the Holland coast are in general coarser than along the Wadden coast. At Noordwijk, the surface sediment at the shoreface and in the adjacent trough is moderately to poorly sorted and contains mud. The latter is likely related to the mud transport along the Holland coast. The sand at the ridges and sand waves offshore Noordwijk is even coarser. These differences in grain size populations reflect the composition of the subsurface but will be partly obscured by selection during transport.

Measured orbital velocity amplitudes at the seabed at 14–16 m depth exceeded 1 m per second during high wave events. This caused high sediment mobility under sheet-flow conditions with abundant sediment suspension at the lower shoreface. Measured ripple dimensions turned out to be controlled by waves, with lower and shorter ripples for higher waves. These observations clearly indicate significant sediment mobility at the lower shoreface under higher wave events. It is yet unclear what this means for the net sand transport.

Calculation of sand transport over the lower shoreface indicates an annual shoreward transport over the 20m depth contour of 3.6 $\pm$ 0.9 million $m^3$. The cross-shore transports increase with decreasing water depth due to increased sediment stirring by waves and increased wave-related sand transport. Including return flow would reduce the annual transports with c. 0.6 million $m^3$. A first calculation shows that storms increase the cumulative long- and cross-shore transports per year considerably.

The results of this study show that the deposits, seabed sediments and morphology, and hydrodynamics at the lower shoreface and inner shelf of the Dutch coast show a striking contrast between the Wadden area and the Holland coast. Shoreface and seabed sediments along the Holland coast are in general coarser grained, wave-orbital velocities reach high values under high waves at the Wadden coast. Holocene 'stiff' layers at Terschelling and Noordwijk display themselves in the shoreface morphology and probably play a role in cross-shore flow and sediment transport. The sediment dynamics suggested by smaller-scale morphological phenomena need further confirmation.

### *5.2. Recommendations for future work*

1. The multibeam surveys revealed unexpected details such as geology-based shoreface gullies and depressions that probably act as conduits for downslope currents and offshore sand transport. The occurrence of these erosional features after a high-wave event suggests large-scale seaward bottom currents and possibly sand transport. It is relevant for coastal management to know if this seaward transport occurs, under which conditions, how large the fluxes are, etc. Therefore, monitoring of near-bed flow strength and direction, and sediment concentrations in these shoreface depressions, to establish the impact of especially high-wave events on the sand budget of the shoreface is recommended.
2. The modelled total yearly landward sand transports over the 16m depth contour consists of a net supply of 3.6 million $m^3$ from the inner shelf and an extra 3.5 million $m^3$ produced by erosion between $-20$ m and $-16$ m. The evolution of the Holland since 1965 coast shows erosion between $-8$ m and $-14$ m. This means that the cross-shore supply from the deeper part of the lower shoreface is by far not sufficient to prevent erosion of its shallower parts. What causes this deepening of the lower shoreface, is not understood. Moreover, it is not clear where the removed sediment volumes ended up. Understanding the sediment fluxes at the shoreface under different conditions is essential for the management of a sandy coast on both short and long timescales. The construction of a sediment budget for the Dutch coast, including the connected tidal basins of the Wadden Sea for the period since 1965 will be a necessary first step to gain insight into the sediment sources and sinks and the net sediment fluxes at decadal timescales. To better understand the sediment budget on century timescales, detailed reconstructions of the Late-Holocene evolution of the Dutch coast are needed.
3. The lack of storm beds at the lower shoreface of Terschelling, as shown by the vibrocores and in contrast to those at the shoreface of Noordwijk, suggests that the Terschelling shoreface is eroding more than that at Noordwijk. This needs to be checked against other sources of information such as a series of depth soundings of the deeper part of the lower shoreface.

## Declaration of competing interest

The authors declare that they have no known competing financial interests or personal relationships that could have appeared to influence the work reported in this paper.

## Data availability

Data will be made available on request.

## Acknowledgements

Many people contributed to the collection and interpretation of the data presented in this paper. The field campaigns were organized by Central Information Technology unit of Rijkswaterstaat. Several colleagues at Deltares helped in handling cores and samples, drawing maps and diagrams and assisted in the writing of reports. Many thanks to all for the support. Harry de Looff and Wout de Vries of Rijkswaterstaat – Traffic and Water Management kept us focussed on the scope of this study. Quirijn Lodder, working at the same department, contributed with data and discussions on the long-term morphodynamics. We thank them for the pleasant cooperation. Reviews by Sytze van Heteren, Quirijn Lodder and an anonymous reviewer greatly improved the paper and are much appreciated.

## Appendix A. Supplementary data

Supplementary data to this article can be found online at https://doi.org/10.1016/j.ocecoaman.2022.106367.

## References

Agaard, T., 2011. Sediment transfer from beach to shoreface: the sediment budget of an accreting beach on the Danish North Sea Coast. Geomorphology 135, 143–157. https://doi.org/10.1016/j.geomorph.2011.08.012.

Agaard, T., 2014. Sediment supply to beaches: cross-shore sand transport on the lower shoreface. J. Geophys. Res.: Earth Surf. 119, 913–926. https://doi.org/10.1002/2013JF003041.

Aigner, T., 1985. Storm Depositional Systems. Dynamic Stratigraphy in Modern and Ancient Shallow-Marine Sequences. Lecture Notes in Earth Sciences, Nr. 3. Springer-Verlag, Berlin, pp. 1–174.

Anthony, E.J., Aagaard, T., 2020. The lower shoreface: morphodynamics and sediment connectivity with the upper shoreface and beach. Earth Sci. Rev. 210, 103334 https://doi.org/10.1016/j.earscirev.2020.103334.

Beets, D.J., van der Spek, A.J.F., 2000. The Holocene evolution of the barrier and the back-barrier basins of Belgium and The Netherlands as a function of late Weichselian morphology, relative sea-level rise and sediment supply. Geol. Mijnbouw/Neth. J. Geosci. 79 (1), 3–16. https://doi.org/10.1017/S0016774600021533.

Beets, D.J., Cleveringa, P., Laban, C., Battegazore, P., 1995. Evolution of the lower shoreface of the coast of Holland between Monster and Noordwijk. Meded. Rijks Geol. Dienst 52, 235–247.

Beets, D.J., van der Valk, L., Stive, M.J.F., 1992. Holocene evolution of the coast of Holland. Mar. Geol. 103, 423–443.

Cleveringa, J., 2000. Reconstruction and modelling of Holocene coastal evolution of the Netherlands. Geol. Ultraiectina 200, 1–197. https://dspace.library.uu.nl/handle/1874/526.

Cowell, P.J., Hanslow, D.J., Meleo, J.F., 1999. The shoreface. In: Short, A.D. (Ed.), Handbook of Beach and Shoreface Morphodynamics. John Wiley & Sons, Chichester, pp. 39–71.

Cowell, P.J., Stive, M.J.F., Niedoroda, A.W., de Vriend, H.J., Swift, D.J.P., Kaminsky, G. M., Capobianco, M., 2003. The Coastal-Tract (Part 1): A conceptual approach to aggregated modeling of low-order coastal change. J. Coast Res. 19 (4), 812–827.

de Haas, T., van der Valk, L., Cohen, K.M., Pierik, H.J., Weisscher, S.A.H., Hijma, M.P., van der Spek, A.J.F., Kleinhans, M.G., 2018. Long-term evolution of the Old Rhine estuary: unravelling effects of changing boundary conditions and inherited landscape. The Depositional Record 5 (1), 84–108. https://doi.org/10.1002/dep2.56.

de Mulder, E.F.J., 1984. Geologische geschiedenis van de Hondsbossche Zeewering. Grondboor Hamer 1984–1, 15–31 (in Dutch).
Ebbing, J.H.J., Laban, C., 1996. Geological history of the area off Walcheren and Zeeuwsch-Vlaanderen (southwestern Netherlands), since the start of the Eemian. Meded. Rijks Geol. Dienst 57, 251–267.
Elias, E., Oost, A., 2021. Morfologische Processen Van Het Friesche Zeegat. Een Conceptueel Model. Report 11205236-003-ZKS-0005. Deltares, Delft.
Elias, E.P.L., Pearson, S.G., van der Spek, A.J.F., Pluis, S., 2022. Understanding meso-scale processes at a mixed-energy tidal inlet: Ameland Inlet, The Netherlands – implications for coastal maintenance. Ocean Coast Manag. 222, 106125 https://doi.org/10.1016/j.ocecoaman.2022.106125.
Elias, E.P.L., van der Spek, A.J.F., 2006. Long-term morphodynamic evolution of Texel Inlet and its ebb-tidal delta (The Netherlands). Mar. Geol. 225, 5–21. https://doi.org/10.1016/j.margeo.2005.09.008.
Elias, E.P.L., van der Spek, A.J.F., 2017. Dynamic Preservation of Texel Inlet, The Netherlands. Understanding the interaction of an ebb-tidal delta with its adjacent coast. Neth. J. Geosci. 96 (4), 293–317. https://doi.org/10.1017/njg.2017.34.
Elias, E.P.L., van der Spek, A.J.F., Lazar, M., 2017. The 'Voordelta', the contiguous ebb-tidal deltas in the SW Netherlands; Large-scale morphological changes and sediment budget 1965-2013; Impacts of large-scale engineering. Neth. J. Geosci. 96 (3), 233–259. https://doi.org/10.1017/njg.2016.37.
Elias, E.P.L., van der Spek, A.J.F., Wang, Z.B., de Ronde, J., 2012. Morphodynamic development and sediment budget of the Dutch Wadden Sea over the last century. Neth. J. Geosci. 91 (3), 293–310. https://doi.org/10.1017/S0016774600000457.
Grasmeijer, B., Schrijvershof, R., van der Werf, J., 2019. Modelling Dutch Lower Shoreface Sand Transport. Report 1220339-005-ZKS-0008. Deltares, Delft. https://puc.overheid.nl/rijkswaterstaat/doc/PUC_634196_31/1/.
Grasmeijer, B., Huisman, B., Luijendijk, A., Schrijvershof, R., van der Werf, J., Zijl, F., de Looff, H., de Vries, W., 2022. Modelling of annual sand transports at the Dutch lower shoreface. Ocean Coast Manag. 217, 105984 https://doi.org/10.1016/j.ocecoaman.2021.105984.
Guillén, J., Hoekstra, P., 1996. The "equilibrium" distribution of grain size fractions and its implications for cross-shore sediment transport: a conceptual model. Mar. Geol. 135, 15–33.
Hamon-Kerivel, K., Cooper, A., Jackson, D., Sedrati, M., Guissado Pintado, E., 2020. Shoreface mesoscale morphodynamics: a review. Earth Sci. Rev. 209, 103330 https://doi.org/10.1016/j.earscirev.2020.103330.
Hijma, M.P., 2017. Geology of the Dutch Coast. The Effect of Lithological Variation on Coastal Morphodynamics. Report 1220040-007-ZKS-0003. Deltares, Delft.
Hijma, M.P., van der Spek, A.J.F., van Heteren, S., 2010. Development of a mid-Holocene estuarine basin, Rhine-Meuse mouth area, offshore The Netherlands. Mar. Geol. 271, 198–211. https://doi.org/10.1016/j.margeo.2010.02.011.
Krämer, K., Holler, P., Herbst, G., Bratek, A., Ahmerkamp, S., Neumann, A., Bartholomä, A., van Beusekom, J.E.E., Holtappels, M., Winter, C., 2017. Abrupt emergence of a large pockmark field in the German Bight, southeastern North Sea. Sci. Rep. 7, 5150. https://doi.org/10.1038/s41598-017-05536-1.
Lodder, Q., Slinger, J., 2022. The 'Research for Policy' cycle in Dutch coastal flood risk management: the Coastal Genesis 2 research programme. Ocean Coast Manag. 219, 106066 https://doi.org/10.1016/j.ocecoaman.2022.106066.
McGinnis, D.F., Schmidt, M., DelSontro, T., Themann, S., Rovelli, L., Reitz, A., Linke, P., 2011. Discovery of a natural $CO_2$ seep in the German North Sea: implications for shallow dissolved gas and seep detection. J. Geophys. Res. 116, C03013 https://doi.org/10.1029/2010JC006557.
Niessen, A.C.H.M., 1989. Project Kustgenese. Geologisch onderzoek van het kustgebied van de Zeeuwse en Zuidhollandse eilanden en de 'gesloten' Hollandse kust. Report Geological Survey of The Netherlands, Haarlem (in Dutch).
Niessen, A.C.H.M., 1990. Project Kustgenese. Geologisch onderzoek van het kustgebied van de Waddeneilanden. Report Geological Survey of The Netherlands, Haarlem (in Dutch).
Niessen, A.C.H.M., Laban, C., 1987. Project Kustgenese, Taakgroep 100. Voortgangsrapportage van het door de Rijks Geologische Dienst uitgevoerde onderzoek 1986/1987 in het kustgebied tussen Castricum en Camperduin. Report Geological Survey of The Netherlands, Haarlem (in Dutch).
Oost, A.P., 1995. Dynamics and sedimentary development of the Dutch Wadden Sea with emphasis on the Frisian Inlet. A study of the barrier islands, ebb-tidal deltas, inlets and drainage basins. Geol. Ultraiectina 126, 1–454.
Oost, A.P., Forzoni, A., van der Spek, A., Vermaas, T., 2019a. Kustgenese-2 'diepe Vooroever'. Core Analysis Noordwijk, Terschelling, Amelander Inlet. Report 1220339-004-ZKS-0008. Deltares, Delft. https://puc.overheid.nl/rijkswaterstaat/doc/PUC_633961_31/1/.
Oost, A.P., Marges, V., Vermaas, T., van Dijk, T., Karaoulis, M., 2019b. Kustgenese-2 'diepe Vooroever'. A Description of the Multibeam Surveys 2017 & 2018. Report 1220339-004-ZKS-0062. Deltares, Delft. https://puc.overheid.nl/rijkswaterstaat/doc/PUC_634166_31/1/.
Passchier, S., Kleinhans, M.G., 2005. Observations of sand waves, megaripples, and hummocks in the Dutch coastal area and their relation to currents and combined flow conditions. J. Geophys. Res.: Earth Surf. 110, 1–15. https://doi.org/10.1029/2004JF000215.
Reineck, H.E., Singh, I.B., 1980. Depositional Sedimentary Environments. Second, Revised and Updated Edition. Springer-Verlag, New York, 549 pp.
Rieu, R., van Heteren, S., van der Spek, A.J.F., de Boer, P.L., 2005. Development and preservation of a mid-Holocene tidal-channel network offshore the western Netherlands. J. Sediment. Res. 75 (3), 409–419.
Schrijvershof, R., Brakenhoff, L., Grasmeijer, B., 2019. Hydrodynamics and Bedforms at the Dutch Lower Shoreface. Analysis of ADCP, ADV and SONAR Observations. Report 1220339-007-ZKS-0009. Deltares, Delft. https://puc.overheid.nl/rijkswaterstaat/doc/PUC_634151_31/1/.
Schroot, B.M., Schüttenhelm, R.T.E., 2003. Expressions of shallow gas in The Netherlands North Sea. Neth. J. Geosci./Geol. Mijnbouw 82 (1), 91–105. https://doi.org/10.1017/S0016774600022812.
Sha, L.P., 1989a. Holocene-Pleistocene interface and three-dimensional geometry of the ebb-delta complex, Texel Inlet, The Netherlands. Mar. Geol. 89, 207–228.
Sha, L.P., 1989b. Geology of the Dutch Shoreface along the Wadden Islands: Application of Shallow Seismic Methods. Report NZ-N-89.21, Rijkswaterstaat, North Sea Directorate, Rijswijk.
Sha, L.P., 1992. Geological Research in the Ebb-Tidal Delta of 'Het Friesche Zeegat'. Report 40010 Project Kustgenese. Geological Survey of The Netherlands, Haarlem.
Sha, L.P., de Boer, P.L., 1991. Ebb-tidal delta deposits along the West Frisian Islands (The Netherlands): processes, facies architecture and preservation. In: Smith, D.G., Reinson, G.E., Zaitlin, B.A., Rahmani, R.A. (Eds.), Clastic Tidal Sedimentology. Memoir 16. Canadian Society of Petroleum Geologists, pp. 199–218.
Sha, L.P., Laban, C., Zonneveld, P.C., 1996. Influence of the Pleistocene topography on the Holocene coastal development off Texel. Meded. Rijks Geol. Dienst 57, 79–95.
van Alphen, J.S.L.J., Damoiseaux, M.A., 1987. A Morphological Map of the Dutch Shoreface and Adjacent Part of the Continental Shelf (1 :250.000). Report Rijkswaterstaat Directie Noordzee NZ-N-87.21/Meetkundige Dienst MDLK-R-87.18.
van Alphen, J.S.L.J., Damoiseaux, M.A., 1989. A geomorphological map of the Dutch shoreface and adjacent part of the continental shelf. Geol. Mijnbouw 68, 433–445.
Van de Meene, J.W.H., Boersma, J.R., Terwindt, J.H.J., 1996. Sedimentary structures of combined flow deposits from the shoreface-connected ridges along the central Dutch coast. Mar. Geol. 131, 151–175.
Van de Meene, J.W.H., 1994. The shoreface-connected ridges along the central Dutch coast. Neth. Geogr Stud. 174, 1–222.
van de Meene, J.W.H., van Rijn, L.C., 2000a. The shoreface-connected ridges along the central Dutch coast - part 1: field observations. Continent. Shelf Res. 20, 2295–2323.
van de Meene, J.W.H., van Rijn, L.C., 2000b. The shoreface-connected ridges along the central Dutch coast - part 2: morphological modelling. Continent. Shelf Res. 20, 2325–2345.
van der Hout, C.M., Gerkema, T., Nauw, J.J., Ridderinkhof, H., 2015. Observations of a narrow zone of high suspended particulate matter (SPM) concentrations along the Dutch coast. Continent. Shelf Res. 95, 27–38. https://doi.org/10.1016/j.csr.2015.01.002.
van der Spek, A.J.F., 1997. De geologische opbouw van de ondergrond van het mondingsgebied van de Westerschelde en de rol hiervan in de morfologische ontwikkeling. TNO report NITG-97-284-B. Netherlands Institute of Applied Geosciences TNO - *National Geological Survey*, Utrecht (in Dutch).
van der Spek, A.J.F., Elias, E.P.L., 2021. Half a century of morphological change in the Haringvliet and Grevelingen ebb-tidal deltas (SW Netherlands) - impacts of large-scale engineering 1964-2012. Mar. Geol. 432, 106404 https://doi.org/10.1016/j.margeo.2020.106404.
van der Spek, A., Lodder, Q.J., 2015. A new sediment budget for The Netherlands; the effect of 15 years of nourishing (1991-2005). In: Proceedings Coastal Sediments 2015, San Diego, CA, 11-14 May 2015. World Scientific, 12 pp.
van der Spek, A.J.F., Cleveringa, J., van Heteren, S., van Dam, R.L., Schrijver, B., 1999. Reconstructie van de ontwikkeling van de Hollandse Kust in de laatste 2500 jaar, TNO report NITG 99-143-A. Netherlands Institute of Applied Geosciences TNO - *National Geological Survey*, Utrecht (in Dutch). https://puc.overheid.nl/rijkswaterstaat/doc/PUC_142776_31/1/.
van der Spek, A., Forzoni, A., Vermaas, T., 2022. Holocene deposits at the lower shoreface and inner shelf of the Dutch coast. Ocean Coast Manag. 224, 106203 https://doi.org/10.1016/j.ocecoaman.2022.106203.
van der Spek, A., van der Werf, J., Grasmeijer, B., Oost, A., Schrijvershof, R., Vermaas, T., 2020. The Kustgenese 2.0 Atlas of the Dutch Lower Shoreface. Report 1220339-000-ZKS-0068. Deltares, Delft. https://puc.overheid.nl/rijkswaterstaat/doc/PUC_632830_31/1/.
van der Valk, L., 1996. Coastal barrier deposits in the central Dutch coastal plain. Meded. Rijks Geol. Dienst 57, 133–199.
van der Werf, J., Álvarez Antolínez, J.A., Brakenhoff, L., Gawehn, M., den Heijer, K., de Looff, H., van Maarseveen, M., Meijer-Holzhauer, H., Mol, J.W., Pearson, S., van Prooijen, B., Santinelli, G., Schipper, C., Tissier, M., Tonnon, P.K., de Vet, L., Vermaas, T., Wilmink, R., de Wit, F., 2019. Data Report Kustgenese 2.0 Measurements. Report 1220339-015-ZKS-0004. Deltares, Delft.
van der Werf, J., Grasmeijer, B., Hendriks, E., van der Spek, A., Vermaas, T., 2017. Literature Study Dutch Lower Shoreface. Report 1220339-004-ZKS-001. Deltares, Delft. https://puc.overheid.nl/rijkswaterstaat/doc/PUC_634161_31/1/.
van der Werf, J.J., Schrijvershof, R.A., Brakenhoff, L.B., Grasmeijer, B.T., 2022. Observations of near-bed orbital velocities and small-scale bedforms on the Dutch lower shoreface. Ocean Coast Manag. 218, 106012 https://doi.org/10.1016/j.ocecoaman.2021.106012.
van Heteren, S., van der Spek, A.J.F., 2003. Long-term Evolution of a Small Estuary: the Lauwerszee (Northern Netherlands). TNO Report NITG 03-108-A. Netherlands Institute of Applied Geosciences TNO - National Geological Survey, Utrecht.
van Heteren, S., van der Spek, A.J.F., 2008. Waar is de delta van de Oude Rijn? Grondboor Hamer 62 (3/4), 72–76 (in Dutch).
van Heteren, S., Baptist, M.J., van Bergen Henegouw, C.N., van Dalfsen, J.A., van Dijk, T.A.G.P., Hulscher, S.J.M.H., Kaag, N.H.B.M., Knaapen, M.A.F., Lewis, W.E., Morelissen, R., Passchier, S., Penning, W.E., Storbeck, F., van der Spek, A.J.F., van het Groenewoud, H., Weber, A., 2003. Delft Cluster – Eco-Morphodynamics of the Seafloor: Final Report. Report 03.01.05-04, Delft Cluster, Delft.
van Heteren, S., van der Spek, A.J.F., de Groot, T.A.M., 2002. Architecture of a Preserved Holocene Tidal Complex Offshore the Rhine-Meuse River Mouth, The Netherlands.

TNO Report NITG 01-027-A. Netherlands Institute of Applied Geosciences TNO - *National Geological Survey*, Utrecht.

van Heteren, S., van der Spek, A., van der Valk, B., 2011. Evidence and implications of middle- to late-Holocene shoreface steepening offshore the western Netherlands. Proceedings Coastal Sediments 2011, 188–201.

van Prooijen, B.C., Tissier, M.F.S., de Wit, F.P., Pearson, S.G., Brakenhoff, L.B., van Maarseveen, M.C.G., van der Vegt, M., Mol, J.W., Kok, F., Holzhauer, H., van der Werf, J.J., Vermaas, T., Gawehn, M., Grasmeijer, B., Elias, E.P.L., Tonnon, P.K., Santinelli, G., Antolínez, J.A.A., de Vet, P.L.M., Reniers, A.J.H.M., Wang, Z.B., den Heijer, C., van Gelder-Maas, C., Wilmink, R.J.A., Schipper, C.A., de Looff, H., 2020. Measurements of hydrodynamics, sediment, morphology and benthos on Ameland ebb-tidal delta and lower shoreface. Earth Syst. Sci. Data 12, 2775–2786. https://doi.org/10.5194/essd-12-2775-2020.

van Rijn, L.C., 1997. Sediment transport and budget on the central coastal zone of Holland. Coast. Eng. 32, 61–90.

van Straaten, L.M.J.U., 1965. Coastal barrier deposits in South- and North-Holland, in particular in the areas around Scheveningen and IJmuiden. In: Mededelingen van de Geologische Stichting, Nieuwe Serie, vol. 17. Haarlem, pp. 41–75.

van Woudenberg, C.C., 1996. De onderwater zanddam bij Loswal Noord: Gedrag en zandtransport. Report NZ-96.03. Rijkswaterstaat North Sea Directorate, Rijswijk (in Dutch).

Verhagen, W., Wiersma, J., 1991. Evaluatie zandstort voor de kust van Wijk aan Zee. Draft report NZ-N-91, Rijkswaterstaat, North Sea Directorate, Rijswijk (in Dutch).

Vermaas, T., 2010. Morphological Behaviour of the Deeper Part of the Holland Coast. Report Deltares/Physical Geography Department - Utrecht University.

Vermaas, T., van Dijk, T., Hijma, M., 2015. Bodemdynamiek van de diepe onderwateroever met oog op de -20 m NAP lijn. Report 1220034-003-ZKS-0002. Deltares, Delft (in Dutch).

Vos, P., van der Meulen, M., Weerts, H., Bazelmans, J., 2020. Atlas of the Holocene Netherlands. Landscape and Habitation since the Last Ice Age. Amsterdam University Press, 96 pp.

Wiersma, J., van Alphen, J.S.L.J., 1988. The morphology of the Dutch shoreface between Hook of Holland and Den Helder (The Netherlands). In: de Boer, P.L., van Gelder, A., Nio, S.D. (Eds.), Tide-Influenced Sedimentary Envionments and Facies. D. Reidel/ Kluwer, Dordrecht, pp. 101–111.